Topological expansion and exponential asymptotics in 1D quantum mechanics

2000 J. Phys. A: Math. Gen. 33 1543

(http://iopscience.iop.org/0305-4470/33/8/304)

J. Phys. A: Math. Gen. **33** (2000) 1543–1580. Printed in the UK PII: S0305-4470(00)03335-7

Topological expansion and exponential asymptotics in 1D quantum mechanics

Stefan Giller

Theoretical Physics Department II, University of Łódź, Pomorska 149/153, 90-236 Łódź, Poland

E-mail: sgiiler@krysia.uni.lodz.pl

Received 12 April 1999, in final form 8 November 1999

Abstract. Borel summable semiclassical expansions in 1D quantum mechanics are considered. These are the Borel summable expansions of fundamental solutions and of quantities constructed with their help. An expansion, called topological, is constructed for the corresponding Borel functions. This allows us to study the Borel plane singularity structure in a systematic way. Examples of such structures are considered for linear, harmonic and anharmonic potentials. Together with the best approximation provided by the semiclassical series the exponentially small contributions completing the approximation are considered. A natural method of constructing such exponential asymptotics based on the Borel plane singularity structures provided by the topological expansion is developed. The method is used to form the semiclassical series including exponential contributions for the energy levels of the anharmonic oscillator.

1. Introduction

In this paper we continue our investigations to represent basic quantities of the quantum mechanics in the form of Balian–Bloch representation, i.e. in the form of the Laplace–Borel transforms in which the conjugate variables are an action and the Planck constant [1]. The key results, which this paper is based on, have been published earlier [2]. The present paper develops these key ideas and, using the explicit form of the fundamental solutions [11, 12] to the 1D Schrödinger equation, expresses the Balian–Bloch representation in the form of what we call a topological expansion. We also describe the way to use the representation to construct extended JWKB approximations in the form of so-called exponential asymptotics (sometimes called also hyperasymptotics, (see [23–28] and references therein) and we also consider some particular applications of the Balian–Bloch method.

For simplicity, the potentials considered in this paper are assumed to be polynomial but the main results are valid for more general meromorphic potentials as well.

Being Borel summable, the fundamental solutions define the corresponding Borel functions by which they can be represented in the form of Borel transformation from the Borel plane of the action variable to the complex plane of the $\overline{h}^{-1}$ variable. For the polynomial potentials these Borel functions are in fact all the same despite the fact that they are defined by different fundamental solutions [3]. This means, of course, that the fundamental solutions themselves are in close relation to each other, being, in fact, a mutual analytical continuation of each other in the $\overline{h}^{-1}$ plane [2, 3].

Therefore, to get any of the fundamental solutions it is only necessary to properly choose an integration path in the Borel plane. However, to do this a detailed knowledge

0305-4470/00/081543+38$30.00

of singularity distribution of the Borel function in the Borel plane is necessary. It is the aim of this paper to provide us with an effective tool for studying these singularities. Namely, we develop an expansion for the Borel function, called toplogical, in which an expansion parameter is the complexity of the Borel plane corresponding to successive terms of the expansion.

With the help of the fundamental solutions we can solve most 1D quantum mechanical problems so that the corresponding quantities involved in the problems considered depend on different pieces of the fundamental solutions used. These quantities themselves can then have semiclassical representations which can be Borel summable and can serve as a source of their semiclassical approximations as well. It is clear that the corresponding Borel plane singularities of these quantities are then defined by the pieces of the fundamental solutions constructing them. Therefore the topological expansion method can also be applied to determine the approximate singularity structure for these quantities.

The semiclassical expansions used as a source of approximations are considered as insufficient, providing us with unavoidable nonvanishing errors. It is well known that the reasons for these errors are due to the divergence of the semiclassical series so that the latter, as asymptotic, neglect the exponentially small contributions. Nevertheless, since the series are Borel summable they have to contain the full information about such exponential contributions. A common approach was simply to recover these contributions, leading to a formulation of so-called resurgent theory [25–28].

Note, however, that the exponentially small contributions have their own importance since in many cases these contributions are *dominant*. The best known such case is the difference between the energy levels of different parities in the symmetric double well [31]. But there are also the cases of transition probabilities in the tunnelling phenomena [31] or their adiabatic limits in the time-dependent problem of transitions between two (or more) energy levels ([33, 34] and references therein) or the exponential decaying of resonances in the weak electric field (see [35, 36] and references therein).

In this paper we make full use of the Borel summability of the quantities considered as well as of the corresponding topological expansions to construct the relevant exponential asymptotics.

However, a necessary step of our formulation is knowledge of the Borel plane singularity structure of any considered quantity. This is simply the topological expansion which allows us to assemble the knowledge step by step.

The toplogical expansion is constructed directly from the Fröman and Fröman representation of the fundamental solutions which themselves are given in the forms of functional series [2–4]. Therefore, we begin in section 2 with a detailed presentation of the series.

In section 3 the topological series representation for the Borel functions is introduced and its convergence is proved. This representation provides us with an algorithm for approximate calculations of Borel functions alternative to the ones based on Padé approximants [5, 8, 9, 14], continued fractions [10] or conformal transformations [14].

In section 4, singularity structures of the topological series expansion are analysed and their hierarchic form (which gives rise to the name of the series) is established. We consider there as the simplest examples the 'first sheet' singularity structures of the linear and harmonic potentials. In particular, we completely describe the singularity structure of the Borel plane of the harmonic oscillator Joos function found first by Voros by a different method [19].

The results obtained in sections 3 and 4 are applied in section 5 where the solution of the so-called connection problem within the framework of the Balian–Bloch representation is discussed.

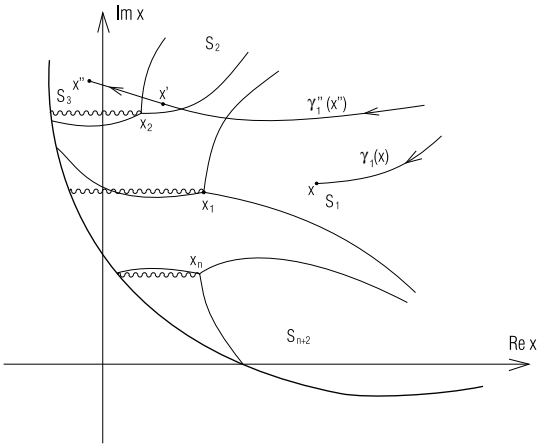

Figure 1. The Stokes graph for a general polynomial potential of nth degree.

In section 6 we discuss the problem of the exponential asymptotics [23–28]. We show that this problem has a natural solution in the framework of the Balian–Bloch representation and gets natural support from the topological expansion method.

In section 7 the energy levels of the single-well anharmonic potential are considered in order to show how to use the topological expansion to construct their extended exponential asymptotics.

Finally, in section 8 we summarize our results.

2. Fundamental solutions

Let us recall the basic notions of our considerations (see [2] for details).

The fundamental solutions satisfy the Schrödinger equation:

$$\Psi''(x, \lambda, E) - \lambda^2 q(x, E)\Psi(x, \lambda, E) = 0 \tag{2.1}$$

where $q(x, E) = V(x) - E$, $\lambda = \sqrt{2m}\hbar^{-1}$. Both λ and the energy E can take on complex values. $V(x)$ is assumed to be a polynomial of any degree $n \geqslant 1$.

A set of fundamental solutions is attached in a unique way to the so-called Stokes graph corresponding to a given polynomial potential $V(x)$. A relevant piece of the graph is shown in figure 1. Each Stokes graph is a collection of lines (Stokes lines) in the complex x-plane which are loci of vanishing of the real parts of actions defined by the integrals $W_i(x, E) = \int_{x_i}^{x} q^{\frac{1}{2}}(y, E)\,\mathrm{d}y$, $i = 1, \ldots, n$, where x_i are roots of $q(x, E)$. In what follows we shall also assume that energy E is in a generic position, i.e. all the roots of $q(x, E)$ are simple. In such a case three Stokes lines emerge from each root, as is shown in figure 1. (A bold line in the figure denotes its technical border.) The wavy lines in the figure denote cuts of the two-sheeted Riemann surface of the x-variable on which $q^{\frac{1}{2}}(x, E)$ is really defined. Because of this there is also another copy of the Stokes lines lying on the second sheet (the latter being not visible, lying below the first one shown in figure 1) which position on the sheet coincides, however, with that of the Stokes lines of the first sheet shown in figure 1.

The fundamental solutions are defined in infinite connected domains called sectors with boundaries of the latter consisting of the Stokes lines and x_i. The sectors of the first sheet are shown in figure 1, where they are denoted by $S_1, S_2, \ldots, S_{n+2}$. The corresponding sectors on the second sheet shall be denoted by $S'_1, S'_2, \ldots, S'_{n+2}$. (Note that a total number of sectors on

each sheet is equal to $n+2$ for a polynomial potential of degree n.) Two fundamental solutions which can be defined in the corresponding sectors S_k and S'_k coincide however (up to a phase factor $\pm i$), representing with the accuracy mentioned the same holomorphic solution to (2.1). Therefore, there are only $n+2$ pairwise independent fundamental solutions.

The above identity of the fundamental solutions defined in the corresponding sectors S_k and S'_k should be held in mind since it is used permanently in this paper in the procedure of the analytical continuation, both in x and λ, of the holomorphic solution represented by each of these two fundamental solutions.

The following fundamental solution $\Psi_1^\sigma(x,\lambda,E)$ to (2.1) can be attached to the sector S_1:

$$\Psi_1^\sigma(x,\lambda,E) = q^{-\frac{1}{4}}(x,E)\mathrm{e}^{\sigma\lambda\int_{x_1}^x q^{\frac{1}{2}}(y,E)\,\mathrm{d}y}\chi_1^\sigma(x,\lambda,E) \qquad \mathrm{Re}\left[\sigma\lambda\int_{x_1}^x q^{\frac{1}{2}}(y,E)\,\mathrm{d}y\right] < 0$$
$$x \in S_1 \qquad \sigma = \pm 1 \qquad q(x_1,E) = 0 \tag{2.2}$$

with the 'amplitude factor' $\chi_1^\sigma(x,\lambda,E)$ given by the following functional series:

$$\chi_1^\sigma(x,\lambda,E) = 1 + \sum_{n\geqslant 1}\left(\frac{\sigma}{2\lambda}\right)^n \int_{\gamma_1^\sigma(x)}\mathrm{d}y_1 \ldots \int_{\gamma_1^\sigma(y_{n-1})}\mathrm{d}y_n\omega(y_1)\ldots\omega(y_n)$$
$$\times[1-\mathrm{e}^{2\lambda\xi(y_1,x)}][1-\mathrm{e}^{2\lambda\xi(y_2,y_1)}]\ldots[1-\mathrm{e}^{2\lambda\xi(y_n,y_{n-1})}] \tag{2.3}$$

where

$$\omega(y) = \frac{1}{4}\left[\frac{q''(y)}{q^{\frac{3}{2}}(y)} - \frac{5}{4}\frac{q'^2(y)}{q^{\frac{5}{2}}(y)}\right] = -q^{-\frac{1}{4}}(y)(q^{-\frac{1}{4}}(y))''$$
$$\xi(x_1,x) = -\sigma\int_{x_1}^x q^{\frac{1}{2}}(y,E)\,\mathrm{d}y \tag{2.4}$$

and where an obvious dependence of ω, q, ξ, etc on E has been dropped. We shall also put $\sigma = -1$ in (2.2)–(2.4) assuming that in (2.2) the corresponding inequality is satisfied in this case.

The integration path γ_1^σ in (2.3) starts from the infinity of the sector S_1. The points $x, y_1, \ldots, y_{n-1}$ of the path defining the nth multiple integral in (2.3) are ordered in such a way as to satisfy the condition (2.2) for each ordered pair (y_k, y_{k-1}) taken as the limits of the integral in (2.2). Such a path is called canonical.

The $n+1$ fundamental solutions which can be defined in the remaining sectors of the Stokes graph of figure 1 can be obtained from the solution $\Psi_1(x,\lambda,E)$ by the analytic continuation, both in x and λ.

To get the fundamental solution $\Psi_2(x,\lambda)$, for example, we can continue it in λ rotating the latter clockwise by the angle π. As follows from (2.2) the Stokes lines then rotate counterclockwise around their turning points by the angles $2\pi/3$ reconstructing eventually their initial positions. The sectors follow these rotations in the order $S_1 \to S_2 \to \cdots \to S_{n+2} \to S_1$ so that the infinite end of the path γ_1 (its finite end at the point x is kept, of course, fixed) rotates with S_1 to S_2. The path γ_1 deformed in this way remains however canonical in the corresponding formula (2.2) defining $\Psi_2(x,\lambda)$. Next, if we wish, we can move x from S_1 to S_2 shifting it simply back to S_2 along γ_1.

We can apply the above procedure to obtain $\Psi_{n+2}(x,\lambda)$ as well rotating λ counterclockwise by π.

Therefore, the fundamental solutions $\Psi_2(x,\lambda)$ and $\Psi_{n+2}(x,\lambda)$ are defined in the 'λ-plane' on both the sides of its cut made along the negative half of the real axis whilst $\Psi_1(x,\lambda)$ is defined on the positive half of the latter, see figure 2 (where the wavy line means the corresponding cut).

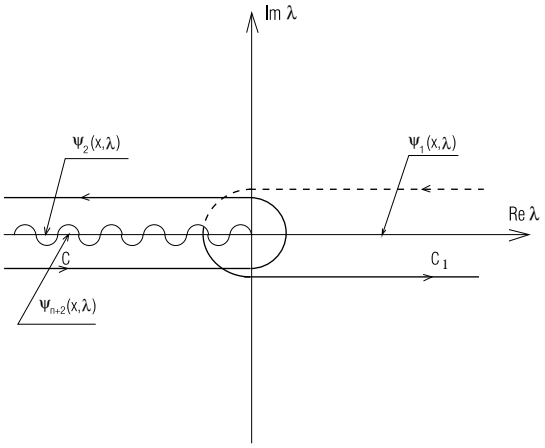

Figure 2. The cut λ-plane corresponding to the solution $\Psi_1(x, \lambda)$ and its analytical continuations in this plane.

Let us note also that to define the fundamental solution in the sector S_1' it is enough to substitute σ in (2.2)–(2.4) by $-\sigma$. Then x is (obviously) unchanged whilst ξ changes its sign.

In the sector S_1 the following semiclassical expansion for $\chi_1(x, \lambda)$ takes place:

$$\chi_1(x,\lambda) \sim \chi_1^{as}(x,\lambda) = 1 + \sum_{n\geqslant 1} \frac{\kappa_{1,n}(x)}{(2\lambda)^n}$$

$$\kappa_{1,n}(x) = \int_{\infty_k}^{x} \mathrm{d}y_n q^{-\frac{1}{4}}(y_k)\left(q^{-\frac{1}{4}}(y_n)\int_{\infty_k}^{y_n} \mathrm{d}y_{n-1} q^{-\frac{1}{4}}(y_{n-1}) \right. \tag{2.5}$$

$$\left. \times\left(\ldots q^{-\frac{1}{4}}(y_2)\int_{\infty_k}^{y_2} \mathrm{d}y_1 q^{-\frac{1}{4}}(y_1)\left(q^{-\frac{1}{4}}(y_1)\right)''\ldots\right)''\right)'' \qquad k = 1, 2, \ldots.$$

As it has been shown in [2] if x stays in S_1 of figure 1 then we can define for $\mathrm{Re}\, s < 0$ the following Laplace transformation of the amplitude factor $\chi_1(x, \lambda)$:

$$\tilde{\chi}_1(x,s) = \frac{1}{2\pi \mathrm{i}}\int_C \mathrm{e}^{-2\lambda s}\frac{\chi_1(x,\lambda)}{\lambda}\,\mathrm{d}\lambda \tag{2.6}$$

with the integration contour C shown in figure 2. (The factor 2 in the exponential function in (2.6) is introduced for convenience.) By the form (2.6) $\tilde{\chi}_1(x, s)$ is defined holomorphically in the half-plane $\mathrm{Re}\, s < \mathrm{Re}\,\xi(x_1, x)$ and since $\mathrm{Re}\,\xi(x_1, x)$ is positive $\tilde{\chi}_1(x, s)$ appears to be, in fact, the Borel transform of $\chi_1(x, \lambda)$. The contour C in (2.6) can be chosen as a circle with its radius λ to be large enough to substitute $\chi_1(x, \lambda)$ by its semiclassical series (2.5). Then for $|s| < |\xi(x_1, x)|$ the lhs of (2.6) can be integrated to give the following Borel series:

$$\tilde{\chi}_1(x,s) = 1 + \sum_{n\geqslant 1}\kappa_{1,n}(x)\frac{(-s)^n}{n!} \tag{2.7}$$

convergent in the circle $|s| < |\mathrm{Re}\,\xi(x_1, x)|$. The point $s_0(x) = \xi(x_1, x)$ is a singularity for $\tilde{\chi}_1(x, s)$ closest to the origin.

The transformations (2.6) can be inverted to give

$$\chi_1(x,\lambda) = 2\lambda\int_{\tilde{C}} \mathrm{e}^{2\lambda s}\tilde{\chi}_1(x,s)\,\mathrm{d}s \tag{2.8}$$

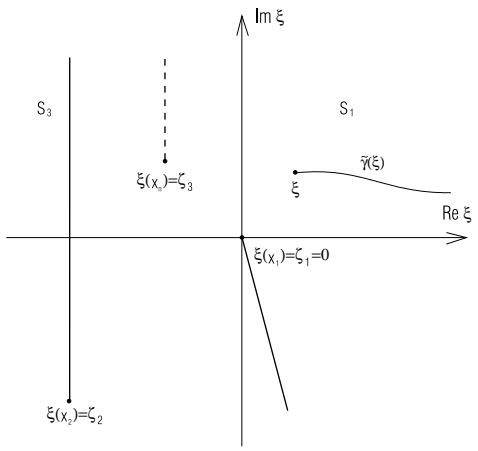

Figure 3. The ξ-plane singularities corresponding to $\tilde{\Phi}_1^{(0)}(\xi, s)$ (case $q = 0$).

where the contour $\tilde{C}$ starts at the infinity $\mathrm{Re}\,(\lambda s) = -\infty$ and ends at $s = 0$. Since $\tilde{C}$ can be freely deformed in the half-plane $\mathrm{Re}\, s \leqslant 0$ the formula (2.8) defines $\chi_1(x, \lambda)$ in the whole sheet shown in figure 2 excluding the points of the negative real half-axis.

The following is worth noting. Formula (2.8) is certainly valid for $\mathrm{Re}\,\lambda > 0$ when the contour $\tilde{C}$ stays in the half-plane $\mathrm{Re}\, s < 0$. It can be continued, however, to other domains of the Riemann λ-surface corresponding to $\chi_1(x, \lambda)$ if accompanied by suitable changes of the variable x. Thus, for example, when continuing x to the sector S_2 and deforming the contour C in figure 2 into C_1 (2.6) will then define $\tilde{\chi}_1(x, s)$ in the half-plane $\mathrm{Re}\, s > 0$. On the other hand, the inverse formula (2.8) defines then $\chi_1(x, \lambda)$ in the half-plane $\mathrm{Re}\,\lambda < 0$ with the contour C in the formula deformed (anticlockwise) from its position in the left half-plane to its new position in the right half of the s-plane. The function $\chi_1(x, \lambda)$ then fulfils for $\lambda > 0$ the condition $\chi_1(x, -\lambda) \equiv \chi_2(x, \lambda)$. Possible singularities of $\tilde{\chi}_1(x, s)$ existing in the corresponding half-plane $\mathrm{Re}\, s > 0$ when x stays in the sector S_1 move to the half-planes $\mathrm{Re}\, s < 0$ when x moves to the sector S_2 (see also section 5 for a relevant discussion).

3. Topological expansion of Borel function $\tilde{\chi}_1(x, s)$

As follows from the definition of $\tilde{\chi}_1(x, s)$, if we want to learn something about it we have to analyse $\chi_1(x, \lambda)$ as given by (2.3). We shall show below that if x stays in S_1 (see figure 1) then it is possible to represent each term of the series in (2.3) in the form of the Laplace transformation, i.e. we shall show that $\tilde{\chi}_1(x, s)$ can also be represented by some convergent functional series. The series, however, can be continued further to the whole x-plane, the latter being deprived of some vicinities of its turning points.

To this end let us consider the nth term of the series in (2.3) and particularly its n-fold integral. Introducing $\xi = \xi(x) = \xi(x_1, x)$ as a new integration variable we get

$$Y_n(\xi, \lambda) = \int_{\tilde{\gamma}_1(\xi)} \mathrm{d}\xi_1 \ldots \int_{\tilde{\gamma}_1(\xi_{n-1})} \mathrm{d}\xi_n \tilde{\omega}(\xi_1) \ldots \tilde{\omega}(\xi_n)(1 - \mathrm{e}^{2\lambda(\xi - \xi_1)}) \ldots (1 - \mathrm{e}^{2\lambda(\xi_{n-1} - \xi_n)}) \tag{3.1}$$

where $\tilde{\omega}(\xi(x)) \equiv \omega(x) q^{-\frac{1}{2}}(x)$ and the path $\tilde{\gamma}_1(\xi)$ starts from $\mathrm{Re}\,\xi = +\infty$ and ends at the point ξ of the ξ-plane.

Let us discuss some basic properties of the transformation $\xi = \xi(x)$. First it maps the two-sheeted Riemann surface which the x-plane actually is into another (in general infinitely sheeted) Riemann surface on which each sector of figure 1 is represented by the right (left) half-planes. In particular, sector S_1 in figure 1 is mapped into the right half of this cut ξ-plane and sectors S_2, S_3 and S_{n+2} into the left ones (see figure 3 where the sectors S_2 and S_{n+2} lie below the sheet shown). Zeros of $q(x)$ which are singular points for $\omega(x)q^{-\frac{1}{2}}(x)$ are also suitably transformed into the corresponding root branch points (of the third degree) of $\tilde{\omega}(\xi)$ on the ξ-Riemann surface (see figure 3 and appendix B). On this surface $\tilde{\omega}(\xi)$ becomes additionally infinitely periodic with its complex periods acting, however, between *different* sheets of the surface. As a result of this an image of each root of $q(x)$ proliferates infinitely on the ξ-Riemann surface with every such copy giving rise to new branch point and sheet. The only exception of the latter rule is the linear potential case the ξ-Riemann surface of which is three-sheeted with a single root branch point of the third degree.

Positions of the Stokes lines in figure 3 depend on $\arg\lambda$. For instance, for the latter argument equal to $0, \pm\pi, \pm 2\pi \ldots$ all the Stokes lines emerging from the branch points $\zeta_1, \zeta_2, \ldots$ are parallel to the imaginary axis keeping their parallelness for any $\arg\lambda$. To avoid, however, the possible confusion of identifying cuts with the Stokes lines plotted in the same figures, the latter are *not* depicted in figures 2 and 3 or on the remaining ones being assumed to be parallel to the imaginary axis on each sheet (this corresponds to the choice $\arg\lambda = 0$).

The bold lines (solid or dashed) in figure 3 denote therefore the *cuts* emerging from the branch points $\zeta_1, \zeta_2, \ldots$. According to a common convention each cut drawn on a given sheet represents two parallel boundaries (edges) of the sheet by which the latter can contact (be 'glued') to the corresponding boundaries of other sheets. The edges themselves are pictures of two different lines of the x-plane along which the action variable ξ has the same value at the corresponding points of the lines. We are free in choosing these lines and in designing the gluing of the corresponding edges so that cuts can have arbitrary, independent of λ and of themselves, directions, depending only on our wish to show the desired parts of sheets in figure 3 that we are interested in. Those actually in the figure were drawn to show the sectors S_1 and S_3. One of these cuts emerging of ζ_2 is a picture of the two Stokes lines emerging of the point x_2 of figure 1 and being the boundary of the sector S_2. That emerging from the point $\zeta_1(=0)$ is a picture of another two lines emerging from the point x_1 in figure 1. Neither of them coincides with any of the Stokes lines. One of these lines runs to the infinity of sector S_1 whilst the other runs to another sector infinity (not shown in figure 1) crossing a strip formed by the Stokes lines coming out from the points x_1 and x_n. Neither coincides with any of the Stokes lines. To show sector S_2 in the figure, for example, we would have to rotate the cut emerging from ζ_2 anticlockwise by π to its new vertical position. However, we could rotate the cut by $\pi/2$ only to the horizontal position to get the pattern where both the sectors are partly visible, S_2 above and S_3 below the cut. But to show sector S_{n+2} together with the branch point ζ_3, we have to rotate the cut emerging from $\zeta_1(=0)$ clockwise by an angle larger than π (to the position between ζ_3 and ξ). Of course, by this operation the sector S_3 and the branch point ζ_2 are screened off. In this way, rotating cuts properly, we can achieve any desired situation.

To complete this discussion let us note a common convention (see [37], for example), of making cuts parallel to imaginary axes too. In such a case the corresponding cut coincides with two different Stokes lines whilst the third Stokes line emerges from the relevant branch point in the direction opposite to that of the cut. Of course, the two 'coinciding' Stokes lines then in fact constitute two parallel edges of the corresponding cut. A convenience of cutting sheets in this way is an easy identification of the definite domains of the sheets with corresponding sectors of the Stokes graph. (For example, two neighbouring sectors with a common Stokes line in figure 3 have to be separated by a cut if this line is not actually chosen as an edge of

this cut.) The inconvenience is, as we mentioned earlier, the risk of mistakenly identifying the cuts made in this way, with the Stokes lines themselves. Nevertheless, when the sheets and the cuts joining them have been designed in this way then fitting the sheets together in a different way is only a matter of actual needs and some imagination.

Opening the brackets in (3.1) we get

$$Y_n(\xi,\lambda) = Y^{(0)}_{n;} + \sum_{2\leqslant 2q\leqslant n}\ \sum_{1\leqslant r_1<\cdots<r_{2q}\leqslant n} Y^{(2q)}_{n;r_1\ldots r_{2q}}(\xi,\lambda)(-1)^{r_1+r_2+r_3+\cdots+r_{2q-1}+r_{2q}} + \sum_{1\leqslant 2q+1\leqslant n}\ \sum_{1\leqslant r_1<\cdots r_{2q+1}\leqslant n} Y^{(2q+1)}_{n;r_1\ldots r_{2q+1}}(\xi,\lambda)(-1)^{r_1+r_2+r_3+\cdots+r_{2q+1}} \tag{3.2}$$

where

$$Y^{(0)}_{n;}(\xi) = \int_{\tilde\gamma_1(\xi)} \mathrm{d}\xi_1 \ldots \int_{\tilde\gamma_1(\xi_{n-1})} \mathrm{d}\xi_n \tilde\omega(\xi_1)\ldots\tilde\omega(\xi_n) = \frac{\Omega^n(\xi)}{n!} \tag{3.3}$$

with

$$\Omega(\xi) = \int_{\tilde\gamma_1(\xi)} \mathrm{d}\eta\tilde\omega(\eta) \tag{3.4}$$

and

$$\begin{aligned} Y^{(2q)}_{n;r_1\ldots r_{2q}}(\xi,\lambda) &= \int_{\tilde\gamma_1(\xi)} \mathrm{d}\xi_1 \ldots \int_{\tilde\gamma_1(\xi_{n-1})} \mathrm{d}\xi_n \tilde\omega(\xi_1)\ldots\tilde\omega(\xi_n)\mathrm{e}^{2\lambda(\xi_{r_1}-\xi_{r_2}+\xi_{r_3}-\cdots+\xi_{r_{2q-1}}-\xi_{r_{2q}})} \\ Y^{(2q+1)}_{n;r_1\ldots r_{2q+1}}(\xi,\lambda) &= \int_{\tilde\gamma_1(\xi)} \mathrm{d}\xi_1 \ldots \int_{\tilde\gamma_1(\xi_{n-1})} \mathrm{d}\xi_n \tilde\omega(\xi_1)\ldots\tilde\omega(\xi_n)\mathrm{e}^{2\lambda(\xi-\xi_{r_1}+\xi_{r_2}-\xi_{r_3}+\cdots+\xi_{r_{2q}}-\xi_{r_{2q+1}})} \\ & q = 1, 2, 3, \ldots . \end{aligned} \tag{3.5}$$

Note that all the integrals in (3.5) are absolutely convergent. Therefore, it should now be obvious that to each integral in (3.5) the following Laplace transformation form can be given:

$$Y^{(q)}_{n;r_1\ldots r_q}(\xi,\lambda) = \int_{\tilde C} \mathrm{d}s\mathrm{e}^{2\lambda s}\tilde Y^{(q)}_{n;r_1\ldots r_q}(\xi,s) \qquad q = 0, 1, \ldots$$

where the integration contour $\tilde C$ starts at $\mathrm{Re}\, s = -\infty$ and ends at $s = 0$ and the Laplace transform $\tilde Y^{(q)}_{n;r_1\ldots r_q}(\xi,s)$ is to be determined. We do this in appendix A. An important observation made there is that it is possible to rearrange the order of terms in the series (2.3) in such a way as to sum it in accordance with the increasing q rather than n—the number of integrations in (3.5). (All these are still possible since the series (2.3) is absolutely convergent.) As a result of such reordering $\chi_1(\xi,\lambda)$ can be represented as the following sum:

$$\begin{aligned} &\chi_1(\xi,\lambda) = 2\lambda\sum_{q\geqslant 0}\chi^{(q)}_1(\xi,\lambda) \\ &\xi\in\tilde S_1 \qquad |\arg\lambda| < \pi \end{aligned} \tag{3.6}$$

where

$$\chi^{(q)}_1(\xi,\lambda) = \int_{\tilde C}\mathrm{d}s\mathrm{e}^{2\lambda s}\tilde\Phi^{(q)}_1(\xi,s) \tag{3.7}$$

with $\tilde\Phi^{(q)}(\xi,s)$, $q\geqslant 0$ given by (A.12) of appendix A and with the contour $\tilde C$ shown in figure 5. Of course, since the series (3.6) is absolutely and uniformly convergent we also have

$$\chi_1(\xi,\lambda) = 2\lambda\int_{\tilde C}\mathrm{d}s\mathrm{e}^{2\lambda s}\tilde\Phi_1(\xi,s) \tag{3.8}$$

with $\tilde\Phi_1(\xi,s)$ given by (A.11) so that the corresponding Laplace transform $\tilde\chi_1(\xi,s)$ defined by (2.6) can be identified as

$$\tilde\chi_1(\xi,s) \equiv \tilde\Phi_1(\xi,s). \tag{3.9}$$

The expansions (3.6) and (A.10) shall be called further topological expansions for the following two reasons:

(1) the higher the term of the series in (A.12), the more complicated is its Riemann surface;
(2) the Riemann surface R_q corresponding to the term $\tilde{\Phi}_1^{(q)}(\xi, s)$ in (A.11) can be reduced to some $R_{q'}$ with $q' < q$ when deprived of some singular points of $\tilde{\Phi}_1^{(q)}(\xi, s)$, i.e. a set Σ_q of all singularities of $\tilde{\Phi}_1^{(q)}(\xi, s)$ includes a set $\Sigma_{q'}$ corresponding to $\tilde{\Phi}_1^{(q)}(\xi, s)$ (see the next section).

3.1. Analytic properties of $\tilde{\chi}_1(\xi, s)$

The analytic properties of $\tilde{\chi}_1(\xi, s)$ are established in section A.3. It follows that the Laplace transform $\tilde{\chi}_1(\xi, s)$ is holomorphic in some vicinity of the point $s = 0$ for $\xi \in \boldsymbol{R}(d'')$. $\boldsymbol{R}(d'')$ is the ξ-Riemann surface deprived of its d''-vicinities of all its singular points, see (A.3): i.e. it is the Borel function (2.7) corresponding to $\chi_1(\xi, \lambda)$. For $\operatorname{Re}\xi > 0$, however, $\tilde{\chi}_1(\xi, s)$ is holomorphic in the half-plane $\operatorname{Re} s < \operatorname{Re}\xi$. Therefore, the asymptotic series constructed for $\chi_1(\xi, \lambda)$ when $\lambda \to \infty$ is Borel summable to the function itself—a result which is in full accordance with the corresponding one obtained in [2] and mentioned in section 2.

4. Singularity structure of $\tilde{\chi}_1(\xi, s)$

Because of (3.10) this is the singularity structure of $\tilde{\Phi}_1(\xi, s)$. This structure is determined by the corresponding singularity structures of $\tilde{\Phi}_1^{(q)}(\xi, s)$ due to (A.10). These structures can be investigated by the analytic continuation procedure of formulae (A.11), (A.12) with respect to s and ξ and are, on their own, determined completely by the corresponding singularity structures of $\tilde{\omega}(\xi)$ and the integrations present in (A.11) and (A.12) (see appendix A). These integrations can give rise to singularities due to the following two mechanisms [13]:

(1) moving singularity of the integrand approaches a fixed limit of the integration or, inversely, a moving limit of an integration approaches a fixed singularity of the integrand (so-called endpoint (EP) singularities);
(2) moving singularity of the integrand approaches some another singularity pinching unavoidably in that way the integration contour (so-called pinch (P) singularities).

In the convolution integrals of formula (A.11) only the functions $\tilde{\omega}(\xi)$ and $\Omega(\xi)$ can give rise to both the (EP and P) singularity mechanisms since a dependence of the integrals on the remaining partners of the convolutions are holomorphic.

From the defining formulae (A.12) and from the ξ-Riemann surface structure on which $\tilde{\omega}(\xi)$ and $\Omega(\xi)$ are defined (this structure was sketched in the previous section) it follows also that even for the simplest cases of first few $\tilde{\Phi}_1^{(q)}(\xi, s)$ their global (ξ, s)-Riemann surface structures are too complicated to be fully handled and only some crude descriptions of them are possible, limited to a few first sheets and a few singularities.

However, in making the corresponding analysis by limiting ourselves to the first few q we are free in deforming the integration contours in (A.12), i.e. the limitation of $\tilde{\gamma}_1(\xi)$ to the canonical choices is no longer valid. This observation is very important and proves that the Borel function $\tilde{\chi}_1(\xi, s)$ constructed initially for the fundamental solution of sector S_1 is universal, i.e. each Borel summable solution to the Schrödinger equation (2.1) can be obtained by the Borel transformation of $\tilde{\chi}_1(\xi, s)$ with a properly chosen integration path in the Borel plane. A discussion of the latter property of the Borel summable solutions and some of its consequences is postponed, however, to another paper [3].

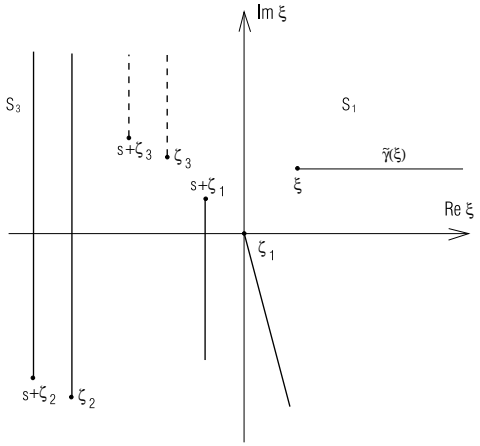

Figure 4. The ξ-plane singularities corresponding to $\tilde{\Phi}_1^{(1)}(\xi, s)$ (case $q = 1$).

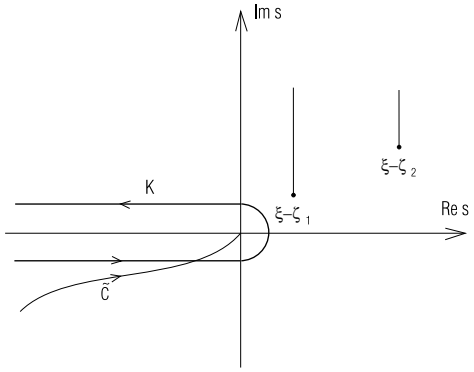

Figure 5. The s-plane singularities corresponding to $\tilde{\Phi}_1^{(1)}(\xi, s)$ (case $q = 1$).

Having in mind the incredible (in general) complexity of the (ξ, s)-Riemann surface structure of $\tilde{\Phi}_1(\xi, s)$ we shall describe first a general procedure for getting this structure for the first few $\tilde{\Phi}_1^{(q)}(\xi, s)$, also taking into account a few singularities of $\tilde{\omega}(\xi)$ and $\Omega(\xi)$, and then we try to give as full a description as possible of such structures for the linear and harmonic potentials.

$q = 0$. It is seen from (A.12) that $\tilde{\Phi}_1^{(0)}(\xi, s)$ is an entire function of s for any ξ not coinciding with singularities of $\tilde{\omega}(\xi)$. Its singularities in the ξ-variable therefore coincide with those of $\Omega(\xi)$ and consequently with those of $\tilde{\omega}(\xi)$ as the EP singularities shown in figure 3.

$q = 1$. This is the Riemann surface structure of $\tilde{\Phi}_1^{(q)}(\xi, s)$ as defined by (A.12) for $q = 1$.

$$\tilde{\Phi}_1^{(1)}(\xi, s) = \int_{\tilde{C}(s)} \mathrm{d}\eta \tilde{\omega}(\xi - \eta)(2s - 2\eta) \frac{I_1([8(s-\eta)\Omega(\xi-\eta) - 4(s-\eta)\Omega(\xi)]^{\frac{1}{2}})}{[8(s-\eta)\Omega(\xi-\eta) - 4(s-\eta)\Omega(\xi)]^{\frac{1}{2}}}. \tag{4.1}$$

It follows from (4.1) that singularities of the subintegral function are essential singularities coniciding with the branch points of $\Omega(\xi)$ and $\Omega(\xi - \eta)$. Because of the single η-integration in (4.1) only the EP mechanism can generate singularities in the 's-plane' since all the η-singularities are moving ones (depending linearly on ξ) so that the positions of all the (essential) singularities of $\tilde{\Phi}_1^{(1)}(\xi, s)$ coincide again with those of $\Omega(\xi - s)$ and $\Omega(\xi)$. Therefore, these positions on the ξ, s Riemann surface are the following:

$$\xi = \zeta_k \qquad \xi - s = \zeta_k \qquad k = 1, 2, \ldots. \tag{4.2}$$

The nature of all these singularities is not altered by the integrations, i.e. all they are branch points. The resulting pattern of cuts on the corresponding Riemann surface which follows from figure 3 is sketched in figures 4 and 5.

In obtaining the pattern of the last figures we have utilized only the singularity structure of the *first* sheet of figure 3. Then the corresponding pattern of the *first* sheet structure of the product $\omega(\xi)\Omega(\xi - \eta)$ (and similar products typical for the subintegral function in (4.1)) has to have the form of figure 4 (where the s variable should be substituted by the η one), i.e. the sheet of figure 4 is the common loci of the branch point singularities of $\omega(\xi)$ and $\Omega(\xi - \eta)$.

The same principles are used in constructing the singularity structures of the corresponding *first* sheets for the case $q = 1$ considered below.

$q = 2$. This is the Riemann surface structure of $\tilde{\Phi}_1^{(2)}(\xi, s)$ as defined by (A.11) for $q = 2$. From (A.14) we have

$$\tilde{\Phi}_1^{(2)}(\xi, s) = \int_{\tilde{C}(s)} \mathrm{d}\eta \int_{\tilde{\gamma}(\xi)} \mathrm{d}\xi_1 \tilde{\omega}(\xi_1 - \eta)\tilde{\omega}(\xi_1)(2s - 2\eta)^2 \frac{I_2(z^{\frac{1}{2}})}{z} \qquad (4.3)$$
$$z = 4(s - \eta)(\Omega(\xi) - 2\Omega(\xi_1) + 2\Omega(\xi_1 - \eta)).$$

Note that the ξ-integration in (4.3) runs across a sheet of the ξ-Riemann surface shown in figure 4 (where the s variable is to be substituted by the η one). However, contrary to the close correspondence between the distributions of sectors and turning points on the Stokes graph of figure 1 and of sheets and the corresponding cuts on figure 3, such a correspondence is lost in the case of figure 4, i.e. we are left only with some properly arranged system of branch points and cuts.

Since half of the cuts in figure 4 are moving (mind the substitution $s \to \eta$) then as well as of the EP singularities, the P singularities are also generated by both the ξ- and η-integrations in (4.3).

Consider first results of the ξ-integration in (4.3).

The EP singularities which follow from this integration coincide (with the corresponding substitution s by η) with those in figures 4 and 5 and are given again by (4.2).

A generation of P singularities can be performed by moving singularities depending on η (see figure 4). For example, moving clockwise the singularity $\eta + \zeta_1$ around the EP ξ of $\tilde{\gamma}_1(\xi)$ and next pinching $\tilde{\gamma}_1(\xi)$ against ζ_1 we generate a singularity of (4.3) at $\eta = 0$ in the η-Riemann surface. It is placed, however, on another sheet of the surface since to achieve it we had to go around the branch point singularity $\xi - \zeta_1$, shown in figure 5, in the clockwise direction.

To obtain all other η-plane singularities generated by the ξ-integration in (4.3) we proceed in the same way. All these singularities lie on sheets which can be reached by going around the two branch points (in any direction—clockwise or anticlockwise) shown in figure 5. Therefore, all these singularities are shared by the actual positions of the branch points cuts of figure 5. They can become visible by cutting the η-plane in a different way or by moving appropriately both the branch points to the left.

Choosing, for example, the last possibility and moving ξ toward the sector S_3 we arrive at the situation shown in figure 6. If ξ and η are moved so that $\mathrm{Re}\,\xi < \mathrm{Re}\,\zeta_2 = \mathrm{Re}\,(\eta + \zeta_1)$ then a further motion of $\eta + \zeta_1$ upwards to the point ζ_2 pinches the path $\tilde{\gamma}_1(\xi)$, producing in that way a singularity at $\eta = \zeta_{21} \equiv \zeta_2 - \zeta_1$. It lies to the right from the cut at $\xi - \zeta_1$ in the 'η-plane' and is therefore screened by the cut just mentioned when $\mathrm{Re}\,\xi > \mathrm{Re}\,\zeta_2$ (see figure 7).

By identical analyses applied to each pair $\eta - \zeta_i$, ζ_j of the singularities lying on the sheet in figure 4, the singularities at $s = \zeta_{ij}$ or at $s = \zeta_{ji} = -\zeta_{ij}$ can be produced, being screened by cuts at $s = \xi - \zeta_j$ or at $s = \xi - \zeta_i$, correspondingly. All the singularities produced in this way are branch points.

According to (4.3) the second, final integration is performed over the η-plane providing $\tilde{\Phi}_1^{(2)}(\xi, s)$ with all its ξ- and s-plane singularities. This integration transforms all the η-singularities obtained by the first (ξ-)integration into the corresponding s-ones (by the EP mechanism) and provides us with additional ξ-singularities by the pinch mechanism. Pinching, for example, the singularity $\xi - \zeta_2$ against ζ_{21} we obtain the ξ-singularity at $\xi = \zeta_2 + \zeta_{21}$ lying on a sheet of the ξ-Riemann surface originated by the branch point at ζ_2 on figure 4. This branch point is screened, of course, by the cut at $\xi = s + \zeta_2$ when $\mathrm{Re}\,s > \mathrm{Re}\,\zeta_{ij}$ (see figure 8).

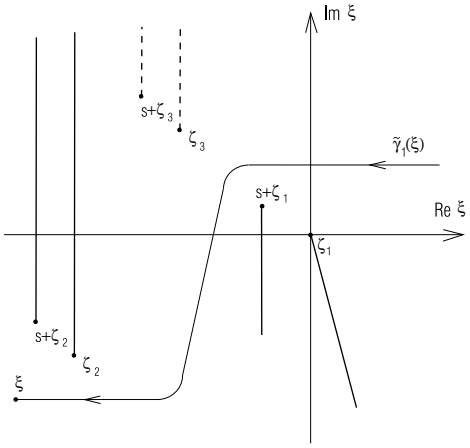

Figure 6. The ξ-plane singularities corresponding to subintegral function in (4.3).

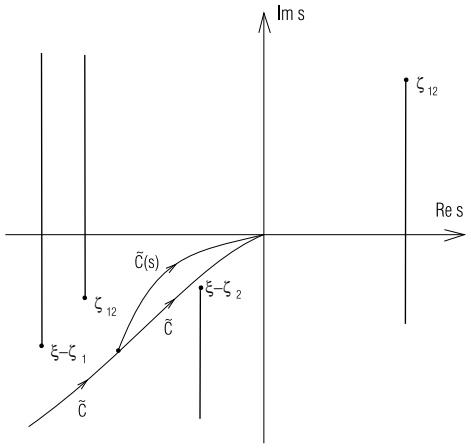

Figure 7. The s-plane singularities corresponding to $\tilde{\Phi}_1^{(2)}(\xi, s)$.

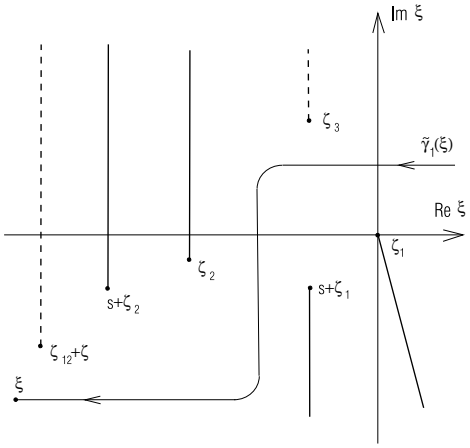

Figure 8. The ξ-plane singularities corresponding to $\tilde{\Phi}_1^{(2)}(\xi, s)$.

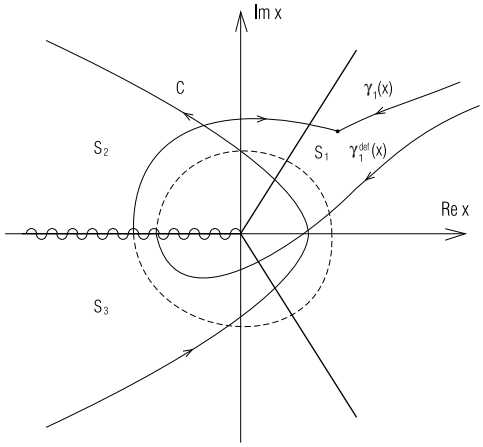

Figure 9. The Stokes graph for the linear potential.

Therefore, figures 7 and 8 show the complete singularity structure of $\tilde{\Phi}_1^{(2)}(\xi, s)$ when continued in ξ in the way shown in figure 6.

4.1. The analytic structure of the Borel function for the linear potential

We can put for this case $q(x, E) \equiv x$ and $\xi = x^{3/2}$ with the corresponding Stokes graph shown in figure 9, and we shall consider $\tilde{\Phi}_1(\xi, s)$ as the Borel function defined by the fundamental solution $\Psi_1(x, \lambda)$.

At first glance the corresponding analysis seems to be simple because of the simplicity of the relevant functions $\tilde{\omega}(\xi) = -\frac{5}{16}\frac{1}{\xi^2}$ and $\Omega(\xi) = \frac{5}{16}\frac{1}{\xi}$ as a result of which the three-sheeted Riemann surface branching at $\xi = 0$ (the surface being the image of the two-sheeted x-plane by the transformation $\xi = x^{3/2}$) decouples into three independent sheets. The unity of the surface is recovered, however, by the solution $\Psi_1(x, \lambda)$, which being holomorphic at $x = 0$

branches at this point as $\xi^{2/3}$ when considered as a function of ξ. However, since we are interested in the properties of the Borel function $\tilde{\Phi}_1(\xi, s)$ determined rather by $\chi_1(\xi, \lambda)/2\lambda$ it is the (ξ, λ)-dependence of the latter function which is most important.

The latter dependence can be established to some extent, noting that the beginning of the integration path $\tilde{\gamma}(\xi)$ in $\chi_1(\xi, \lambda)$ will come back to the infinity of the first sector if the solution $\Psi(\xi, \lambda) = \xi^{-\frac{1}{6}} e^{-\lambda\xi} \chi_1(\xi, \lambda)$ is continued analytically in the λ-plane by rotating λ by the angle $\pm 6\pi$. Of course, the deformed path $\tilde{\gamma}(\xi)$ ends eventually at the point ξ surrounding the latter twice (in the direction suitable to the sign). Naturally, this is exactly the process of analytical continuation described in section 2.

However, as is seen from figure 9, the above λ-continuation of $\chi_1(\xi, \lambda)$ is equivalent to its continuation to the same point ξ along the *deformed* path $\tilde{\gamma}(\xi)$ starting from its initial canonical form. Since by this latter continuation the argument of ξ also changes by $\pm 6\pi$ then the factor $\xi^{-\frac{1}{6}}$ of $\Psi(\xi, \lambda)$ acquires minus by this continuation and so does the factor $\chi_1(\xi, \lambda)$ since by this continuation $\Psi(\xi, \lambda)$ cannot change because it branches at $\xi = 0$ as $\xi^{2/3}$. It therefore follows that $\chi_1(\xi, \lambda)$ branches at $\xi = 0$ as $\xi^{1/6}$.

From the latter observation it follows directly that the Borel function $\tilde{\Phi}_1(\xi, s) (\equiv \tilde{\chi}_1(\xi, s))$ branches at the infinity point of its s-plane also as $s^{1/6}$. This can be seen from the fact that to recover the factor $\chi_1(\xi, \lambda)$ by the Borel transformation of $\tilde{\Phi}_1(\xi, s)$ we have to successively change the integration path in the transformation from the negative real half-axis to the positive one (and vice versa), depending on which sector the infinite end of the deformed path $\tilde{\gamma}(\xi)$ is actually in. These Borel transformation paths are, again, the deformations of each other obtained by moving the infinite end of them along the circle of infinite radius, i.e. all the singularities of $\tilde{\Phi}_1(\xi, s)$ are avoided by these deformations. Since after six such changes the Borel transformation of $\tilde{\Phi}_1(\xi, s)$ has to change its sign in comparison with its initial value, so $\tilde{\Phi}_1(\xi, s)$ itself has to do so also.

Therefore, we conclude that for fixed ξ the s-Riemann surface of $\tilde{\Phi}_1(\xi, s)$ is comprised of six sheets.

The above situation is, however, not so simple when formulae (A.12)–(A.14) defining $\tilde{\Phi}_1(\xi, s)$ are considered. The Bessel functions in these formulae convert the simple pole of $\Omega(\xi)$ at $\xi = 0$ into a corresponding root (of the fourth order) branch points accompanied by essential singularities (see appendix C). Also the successive ξ- and η-integrations in these formulae have to generate unavoidably the branch points at $\xi = 0$, $s = 0$ and $\xi = s$ of the logarithmitic type. This is, of course, because the representation of $\tilde{\Phi}_1(\xi, s)$ given by (A.12)–(A.14) is singular providing us with the correct positions of singularities but not necessarily with their nature. The above example of the linear oscillator shows that the proper behaviour of $\tilde{\Phi}_1(\xi, s)$ close to its singularities is obtained only by the full resummation of these series. Nevertheless, in more complicated cases of potentials, information the series provide us with is certainly very useful, as in the case just considered.

Taking into account the recurrent relations (A.14) we can establish inductively that $\tilde{\Phi}_1(\xi, s)$ being defined by the series (A.11) on its infinitely sheeted (ξ, s)-Riemann surface has on its first two sheets singularities shown in figures 10(*a*) and (*b*) (see appendix C for details). The point $s = 0$ on the sheet of figure 10(*b*) is regular for $\tilde{\Phi}_1(\xi, s)$, according to the general results of appendix A. According to this analysis the points $\xi - s = 0$ are the four order branch points of $\tilde{\Phi}_1(\xi, s)$ and simultaneously its essential singularities but we should have in mind that the last two properties can be incorrect.

The same property concerns the points $\xi = 0$ and $s = 0$, the latter being on the second and further sheets of figure 10(*b*). All these points arrange themselves in the considered approximation of the $\tilde{\Phi}_1(\xi, s)$ infinitely sheeted Riemann surface. However, even for this

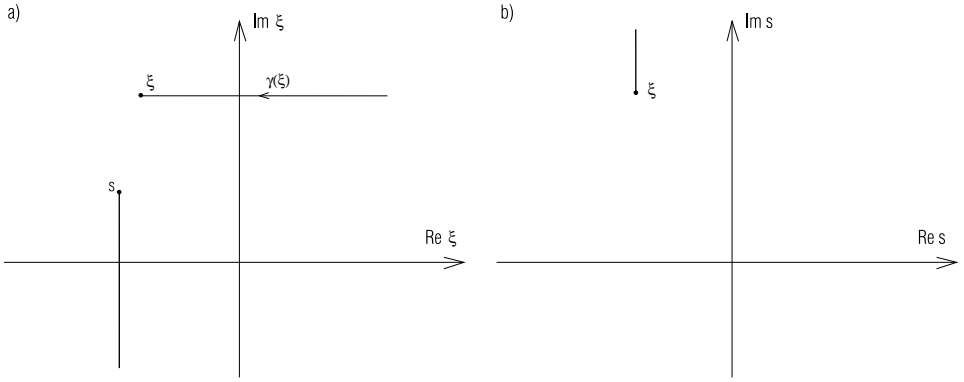

Figure 10. The ξ- and s-plane singularities corresponding to $\tilde{\Phi}_1^{(0)}(\xi, s)$.

simple case, the topology of the surface (apart from its first two sheets) is too complicated to be fully described.

Nevertheless, one general conclusion valid for all the polynomial potentials can be drawn from the above consideration. Namely, if for a general polynomial potential we consider any pair of neighbour sectors joined by the analytic continuation in λ when $\lambda \to \mathrm{e}^{\pm \mathrm{i}\pi}\lambda$ and we continue a fundamental solution defined in one of the sectors to the second along the canonical path then the corresponding 's-plane' singularity structure of the first sheet of the respective Borel function $\tilde{\Phi}_1(\xi, s)$ is exactly the same as for the 'simplest' case of the linear potential described above.

4.2. An alternative non-standard Borel representation for the linear potential wavefunction

In the previous section we noted with disappointment that even in such a simple case as the linear potential, the corresponding Borel function properties which follow from the topological expansion are quite complicated. We have, however, also shown that the actual structure of the linear potential Borel plane should be rather simple. Below, we want to show that this complication is apparent and that a slight change to the definition of the Borel function can greatly simplify the properties for the case considered. Let us replace the definition (2.7) of the Borel function by

$$\tilde{\chi}_1^{\mathrm{alt}}(\xi, \sigma) = \sum_{n \geqslant 0} \frac{(-\sigma)^{n+\frac{1}{2}}}{\Gamma(n + \frac{3}{2})} \kappa_{1,n}(\xi) \tag{4.4}$$

which corresponds to the following representation of $\tilde{\chi}_1^{\mathrm{alt}}(\xi, \sigma)$ by the Laplace transformation:

$$\tilde{\chi}_1^{\mathrm{alt}}(\xi, \sigma) = \frac{1}{\pi \mathrm{i}} \int_{-\mathrm{i}\infty+\lambda_0}^{+\mathrm{i}\infty+\lambda_0} \mathrm{e}^{-2\lambda\sigma} \frac{\chi_1(\xi, \lambda)}{(2\lambda)^{\frac{3}{2}}} \, \mathrm{d}\lambda \tag{4.5}$$
$$0 < \lambda_0 < 1 \qquad \sigma < 0$$

so that the inverse Borel transformation is given by

$$\chi_1(\xi, \lambda) = (2\lambda)^{\frac{3}{2}} \int_{-\infty}^{0} \mathrm{e}^{2\lambda\sigma} \tilde{\chi}_1^{\mathrm{alt}}(\xi, \sigma) \, \mathrm{d}\sigma. \tag{4.6}$$

Let us now make use of the fact that the fundamental solution $\Psi_1(x, \lambda)$ can be given the following integral representation (see [31], mathematical appendix):

$$\Psi_1(x, \lambda) = \frac{\mathrm{i}}{\sqrt{\pi}} (2\lambda)^{\frac{1}{2}} \int_C \mathrm{e}^{\lambda(xy - \frac{y^3}{3})} \, \mathrm{d}y \tag{4.7}$$

where we put x real and positive and the contour C is shown in figure 9.

Changing the integration variable y in (4.7) into $x^{-1/4}y$ and putting $2\sigma = x^{3/4}y - x^{-3/4}y^3/3 + 2x^{2/3}/3$ we can bring the integral to the following form:

$$\Psi_1(x,\lambda) = x^{-\frac{1}{4}}\mathrm{e}^{-\frac{2}{3}\lambda x^{\frac{3}{2}}}\sqrt{\frac{3}{\pi}}(2\lambda)^{\frac{3}{2}}\int_{-\infty}^{0}\mathrm{e}^{2\lambda\sigma}\left[\left(-3\left(\sigma-\frac{1}{3}x^{\frac{3}{2}}\right)x^{\frac{3}{4}}+3x^{\frac{3}{4}}\sqrt{\sigma\left(\sigma-\frac{2}{3}x^{\frac{3}{2}}\right)}\right)^{\frac{1}{3}}\right.$$
$$\left.-\left(-3\left(\sigma-\frac{1}{3}x^{\frac{3}{2}}\right)x^{\frac{3}{4}}-3x^{\frac{3}{4}}\sqrt{\sigma\left(\sigma-\frac{2}{3}x^{\frac{3}{2}}\right)}\right)^{\frac{1}{3}}\right]\mathrm{d}\sigma. \tag{4.8}$$

Hence for $\tilde{\chi}_1^{\mathrm{alt}}(\xi,\sigma)$ we get finally

$$\tilde{\chi}_1^{\mathrm{alt}}(\xi,\sigma) = \sqrt{\frac{3}{\pi}}\left[\left(-3\left(\sigma-\frac{1}{2}\xi\right)\left(\frac{3}{2}\xi\right)^{\frac{1}{2}}+3\left(\frac{3}{2}\xi\right)^{\frac{1}{2}}\sqrt{\sigma(\sigma-\xi)}\right)^{\frac{1}{3}}\right.$$
$$\left.-\left(-3\left(\sigma-\frac{1}{2}\xi\right)\left(\frac{3}{2}\xi\right)^{\frac{1}{2}}-3\left(\frac{3}{2}\xi\right)^{\frac{1}{2}}\sqrt{\sigma(\sigma-\xi)}\right)^{\frac{1}{3}}\right]. \tag{4.9}$$

It follows from (4.9) that $\tilde{\chi}_1^{\mathrm{alt}}(\xi,\sigma)$ is defined on the *two*-sheeted Riemann surface having the branch points $\sigma = 0$ and $\sigma = \xi$ as its unique singularities.

The non-standard representation (4.5), (4.6) of the Borel function considered above shows that the complicated form (2.7) of the standard one depends on the representation itself and it can be simplified greatly by the proper choice of such a representation.

4.3. The singularity structure of the Borel function for the harmonic oscillator

Making, if necessary, a suitable rescaling we can put in this case $q(x) = x^2 + 1$ (assuming the energy to be negative). The corresponding Stokes graph is then shown in figure 11 and we choose as usual the sector S_1 to provide us with the fundamental solution $\Psi_1(x,\lambda)$ and its Borel function $\tilde{\Phi}_1(\xi,s)$. Because of the last conclusion of section 4.1 we consider now a case of the Riemann surface structure corresponding to $\tilde{\Phi}_1(\xi,s)$ when $\xi(\equiv\int_{-i}^{x}\sqrt{y^2+1}\,\mathrm{d}y)$ is continued to sector S_3 of figure 11 (along a canonical path). The first sheets of $\tilde{\Phi}_1^{(1)}(\xi,s)$ and $\tilde{\Phi}_1^{(2)}(\xi,s)$ are shown in figures 12 and 13 respectively.

Again using (A.14) we can show inductively that the first sheets of $\tilde{\Phi}_1^{(2q)}(\xi,s)$ and $\tilde{\Phi}_1^{(2q+1)}(\xi,s)$ are as in figures 14 and 15. All the detailed considerations establishing this can be found in appendix C.2.

4.4. Borel plane structure of harmonic oscillator Joos function

When, in the consideration of the previous section, we push $\mathrm{Re}\,\xi$ to minus infinity (this corresponds to push x to the infinite point ∞_3 of sector S_3 of figure 11) then we get the 'Borel plane' singularity structure of the so-called Joos function for the harmonic oscillator. This is the name given to the coefficient $\chi_{1\to3}(\lambda) \equiv \lim_{\xi\to\infty_3}\chi_1(\xi,\lambda)$ [19] such that the energy spectrum of the harmonic oscillator is given by $\chi_{1\to3}(\lambda) = 0$. Note that in the limit $\xi\to\infty_3$ all the functions $\tilde{\Phi}_1^{(2q+1)}(\xi,s)$ vanish so that the corresponding limiting functions $\tilde{\Phi}_{1\to3}^{(2q)}(s)$ contribute only to $\tilde{\chi}_{1\to3}(s)$.

As follows from the considerations of the previous section, the singularity structure of the latter function is determined by the branch points distributed along the imaginary axes of the s-Riemann surface. This distribution can be described completely, if instead of the Borel function $\tilde{\chi}_{1\to3}(s)$, we consider the one corresponding to $\log\chi_{1\to3}(\lambda)$. To this end let us note that, as follows from figure 11(*a*) the normal sector of $\chi_{1\to3}(\lambda)$ (i.e. the one

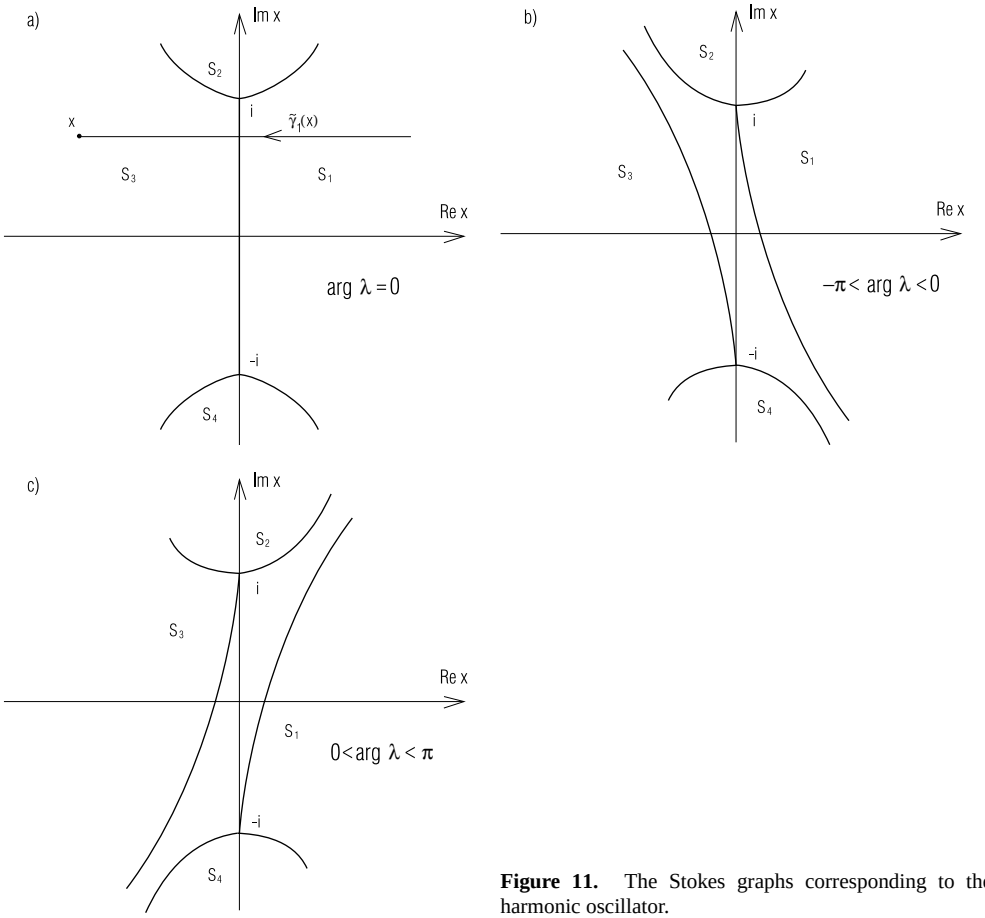

Figure 11. The Stokes graphs corresponding to the harmonic oscillator.

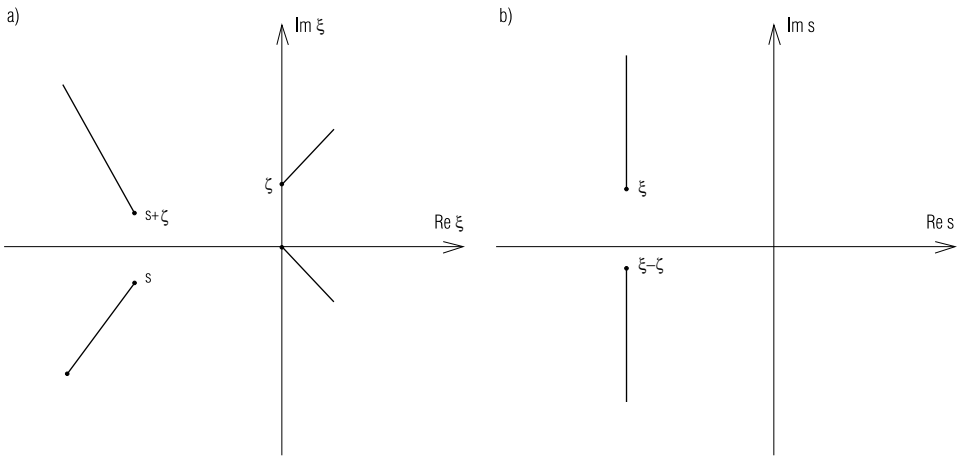

Figure 12. The 'first sheets' singularities of $\tilde{\Phi}_1^{(1)}(\xi, s)$ for the harmonic potential.

where $\chi_{1\to 3}(\lambda)$ is holomorphic and can be expanded into the semiclassical series (2.5)) is defined by $|\arg\lambda| < \pi$. One can easily find also (by analytic continuation in λ)

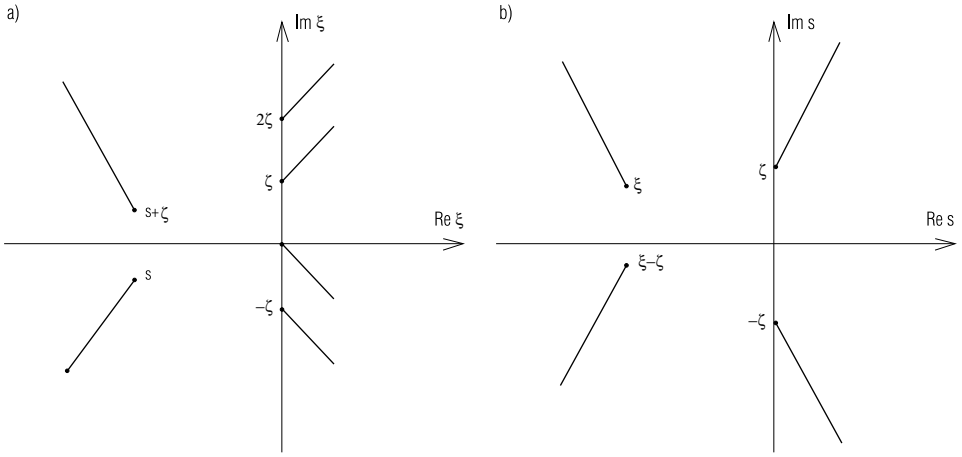

Figure 13. The 'first sheets' singularities of $\tilde{\Phi}_1^{(2)}(\xi, s)$ for the harmonic potential.

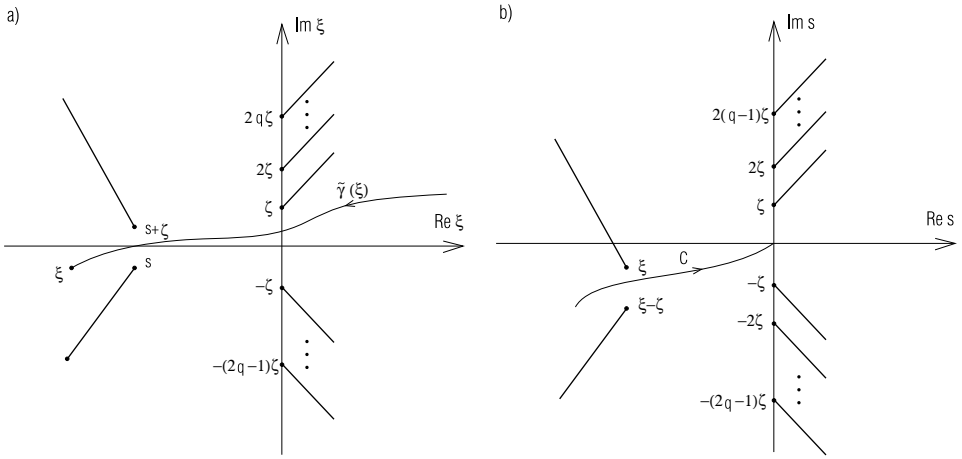

Figure 14. The 'first sheets' singularities of $\tilde{\Phi}_1^{(2q)}(\xi, s)$ for the harmonic potential.

that

$$\chi_{2\to 4}^{\sigma}(\lambda) = \chi_{1\to 3}(\lambda e^{i\sigma\pi}) \qquad 0 < |\arg\lambda| < \pi \tag{4.10}$$

where $\sigma = \arg\lambda/|\arg\lambda|$ and $\chi_{2\to 4}^{\mp}(\lambda)$ are the canonical coefficients corresponding to the graphs of figure 11(*b*) and (*c*) respectively. Despite (4.10), these two canonical coefficients obey the following two other relations:

$$\begin{aligned} &\chi_{1\to 3}(\lambda)\chi_{2\to 4}^{-}(\lambda) = 1 + e^{\pi i\lambda} \qquad 0 < \arg\lambda < \pi \\ &\chi_{1\to 3}(\lambda)\chi_{2\to 4}^{+}(\lambda) = 1 + e^{-\pi i\lambda} \qquad -\pi < \arg\lambda < 0 \end{aligned} \tag{4.11}$$

in which the fact that $2\int_{-i}^{i}\sqrt{y^2+1}\,dy = \pi i$ has been used.

The relations (4.11) follow as a result of an identity which the four fundamental solutions Ψ_k, $k = 1, \ldots, 4$, corresponding to the Stokes graphs of figure 11 have to satisfy since only two of them can be linearly independent.

Using (4.10) we get from (4.11)

$$\chi_{1\to 3}(\lambda)\chi_{1\to 3}(\lambda e^{-i\sigma\pi}) = 1 + e^{\pi i\sigma\lambda} \tag{4.12}$$

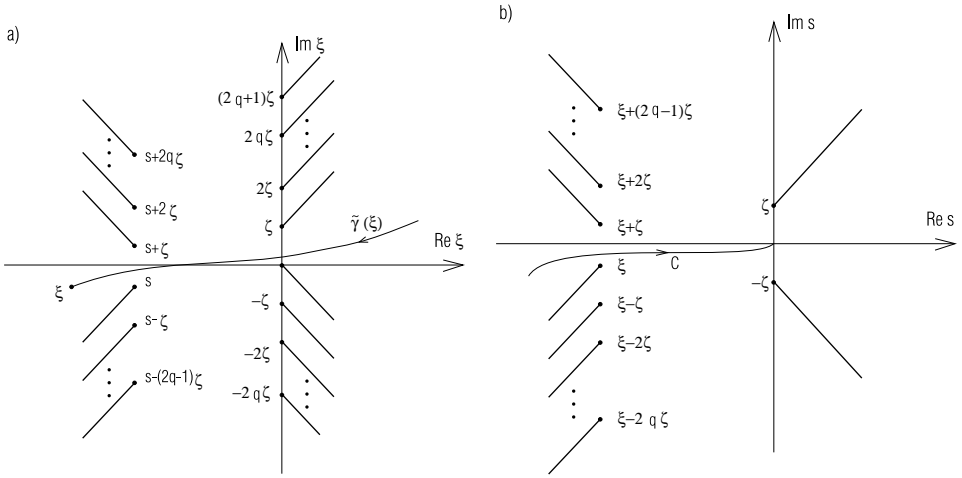

Figure 15. The 'first sheets' singularity structure of $\tilde{\Phi}_1^{(2q+1)}(\xi, s)$ for the harmonic potential.

where $\sigma = \arg\lambda/|\arg\lambda|$ and $0 < |\arg\lambda| < \pi$.

Formula (2.6) can now be used directly to define the Laplace transform $\tilde{\chi}_{1\to3}(s)$ of the Joos function $\chi_{1\to3}(\lambda)$ with the integration contour C_{13} running around the negative half of the real axis of the λ-plane. In this way $\tilde{\chi}_{1\to3}(s)$ is defined by (2.6) as the holomorphic function in the half-plane $\mathrm{Re}\, s < 0$.

The analytic structure of $\tilde{\chi}_{1\to3}(s)$ can, however, be best handled if we consider $\log^*\tilde{\chi}_{1\to3}(s)$ rather than the function itself [19]. Thus, we have

$$\log^*\tilde{\chi}_{1\to3}(s) = \frac{1}{2\pi\mathrm{i}}\int_{C_{13}} \mathrm{e}^{-2\lambda s}\log\chi_{1\to3}(\lambda)\,\mathrm{d}\lambda \tag{4.13}$$

and we can use (4.12) to calculate (4.13) exactly. (Note that $\chi_{1\to3}(\lambda)$ does not vanish in the λ-plane cut along the negative half of the real axis.) Using (4.12) we have

$$\begin{aligned}\log^*\tilde{\chi}_{1\to3}(s) = {} & \frac{1}{2\pi\mathrm{i}}\int_{C^u(\lambda_0)} \mathrm{e}^{-2\lambda s}\log(1+\mathrm{e}^{\pi\mathrm{i}\lambda})\,\mathrm{d}\lambda + \frac{1}{2\pi\mathrm{i}}\int_{C^d(\lambda_0)} \mathrm{e}^{-2\lambda s}\log(1+\mathrm{e}^{-\pi\mathrm{i}\lambda})\,\mathrm{d}\lambda \\ & + \frac{1}{2\pi\mathrm{i}}\int_{C_{13}(\lambda_0)} \mathrm{e}^{-2\lambda s}\log\chi_{1\to3}(-\lambda)\,\mathrm{d}\lambda \end{aligned} \tag{4.14}$$

where $C_{13}(\lambda)$ is one of the contours C_{13} crossing the real axis at $\lambda_0 > 0$ and $C^u(\lambda_0)$, $C^d(\lambda_0)$ are parts of it lying above and below of the real axis correspondingly.

Performing the integrations in the first two integrals in (4.14) (by expanding the logarithms) and changing λ into $-\lambda$ in the third one we get

$$\begin{aligned}\log^*\tilde{\chi}_{1\to3}(s) = {} & \frac{1}{4\pi\mathrm{i}}\sum_{n\leqslant 1}\frac{(-1)^{n+1}}{n}\left\{\frac{\mathrm{e}^{\pi\mathrm{i}n\lambda_0}}{s-\frac{\mathrm{i}\pi n}{2}} - \frac{\mathrm{e}^{-2\pi\mathrm{i}n\lambda_0}}{s+\frac{\mathrm{i}\pi n}{2}}\right\}\mathrm{e}^{-2\lambda_0 s} \\ & + \frac{1}{2\pi\mathrm{i}}\int_{C'(\lambda_0)} \mathrm{e}^{2\lambda s}\log\chi_{1\to3}(\lambda)\,\mathrm{d}\lambda \end{aligned} \tag{4.15}$$

where $C'(\lambda_0)$ is the contour encircling (anticlockwise) the point $\lambda = 0$ and starting and ending at the point $\lambda = -\lambda_0$ of the real axis. Since the right-hand side of (4.15) is independent of λ_0, it can be calculated at $\lambda_0 \to 0$. It can be shown (see appendix E) that the integral in (4.15)

vanishes in this limit and therefore we finally get

$$\log^* \tilde{\chi}_{1\to 3}(s) = \frac{1}{2}\sum_{n\geqslant 1}\frac{(-1)^{n+1}}{s^2+\frac{n^2\pi^2}{4}} = \frac{1}{2\mathrm{i}s}\left(\frac{1}{2\mathrm{i}s}-\frac{1}{\sin(2\mathrm{i}s)}\right). \tag{4.16}$$

The result (4.16) was essentially established by Voros [19] but here it is obtained directly by the definition (4.13) of the Laplace transform for $\log \chi_{1\to 3}(\lambda)$. The inverse transformation can also be performed to give the known expression for $\chi_{1\to 3}(\lambda)$ [19].

Summarizing, one can see that despite the clear way of obtaining corresponding singularity patterns and the underlying structures of the Riemann surfaces they both still become more and more complicated with increasing q. The following main observations follow, however, from the analysis:

(1) The set Σ_{q+1} of singularities corresponding to $\tilde{\Phi}_1^{(q+1)}(\xi, s)$ contains the set Σ_q of these corresponding to $\tilde{\Phi}_1^{(q)}(\xi, s)$.
(2) The new singularities which belong to $\Sigma_{q+1} \setminus \Sigma_q$ are generated on the sheets originated by the singularities of S_q; the latter is true both on the ξ- and on the s-planes.

The following comment concerning the positions of the singularities themselves and their relation to the Feynman path integral is in order. From the above discussion it is seen that these positions are determined by the values of the classical action the latter takes on along suitable classical paths corresponding to the case considered. The paths are real as well as complex (i.e. they are real or complex solutions to the classical equation of motion). They contribute to calculated quantities $\tilde{\Phi}_1^{(q)}(\xi, s)$, $q \geqslant 0$ in the hierarchical way described above so that a path with greater absolute value of the real part of the corresponding action contributes to the later term $\tilde{\Phi}_1^{(q)}(\xi, s)$ of the topological expansion. In this way the latter expansion reflects its close relation to the semiclassical expansion based on the Feynman path integral and the saddle-point technique as well as confirming the role of complex classical paths in such calculations [15–18].

5. An application: the connection problem

The connection problem is an old problem of the JWKB theory which in the context of the Balian–Bloch representation was considered first by Voros [19]. We shall discuss this problem within the framework of our formalism to show the equivalence of the solution it provides with the corresponding method used in our earlier papers (see, for example, [12, 22, 29]).

The main question is how the JWKB formula, being a good approximation to a given solution in some domain of the x-plane, should be changed (in order to still remain a good approximation of the solution) when the solution is continued analytically to another domain of the x-plane. The problem can be solved in many different ways depending on the type of the considered solutions (see, for example, [20–22, 29]). In particular, it can be solved with the aid of fundamental solutions (see [12] for the relevant procedure in an application to matrix element evaluations in JWKB approximation).

In the framework of the Balian–Bloch representation the solution of the problem is the following. Consider the fundamental solution to (2.1) given by (2.2)–(2.4) and continued along a path γ_1'' to the sector S_2 (see figure 2). As follows from the previous section's analysis, continuing analytically along the considered path we cannot meet singularities above the corresponding path $\tilde{\gamma}_1(\xi)$ in the ξ-plane and, therefore, the singularity pattern of $\tilde{\chi}_1(\xi, s)$ in the s-plane is as in figure 16(a), i.e. there are only two cuts on the relevant sheet. Since the integration along $\tilde{C}$ is limited only to lie in the left half-plane we can deform it freely in this

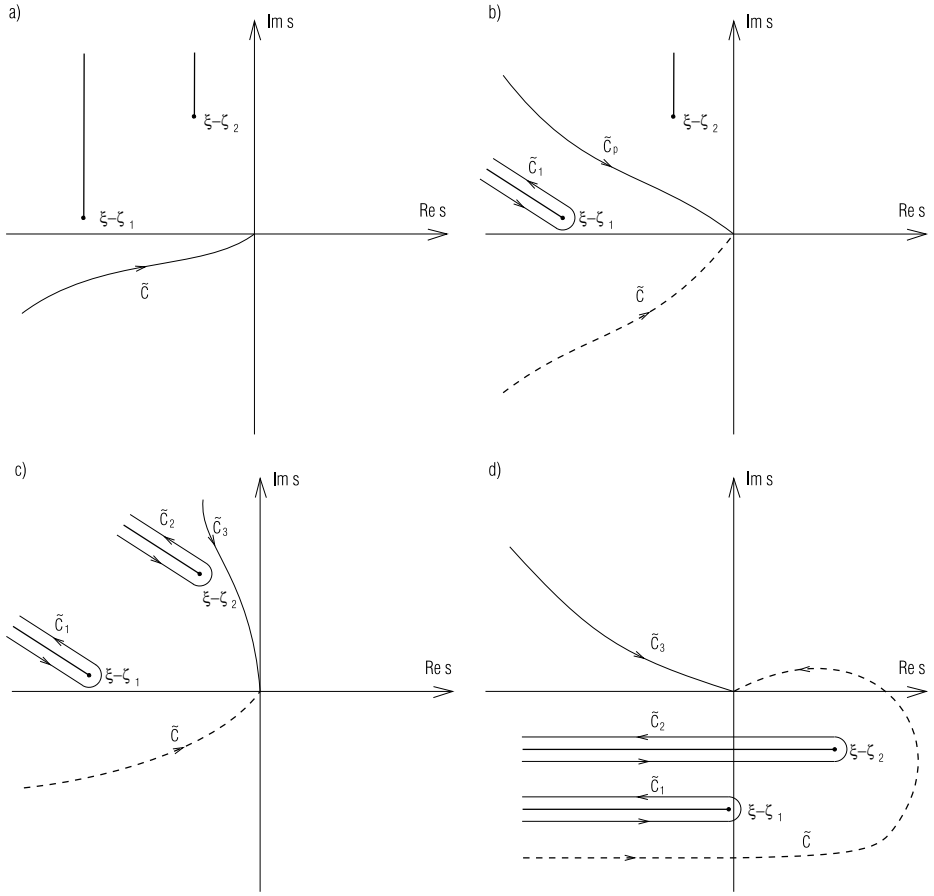

Figure 16. The Borel plane singularities corresponding to $\tilde{\chi}_1^-(\xi, s)$.

half-plane to the position $\tilde{C}_3$, for example (see figure 16(*c*)). But doing this we have to also integrate along the cuts, starting at the points $s = \xi - \zeta_1$ and $s = \xi - \zeta_1$, respectively. Thus, $\psi_1(\xi, \lambda)$ is represented in this way as the following sum:

$$\begin{aligned}\psi_1(\xi, \lambda) &= 2q^{-\frac{1}{4}}(\xi)\mathrm{e}^{-\lambda\xi}\int_{\tilde{C}} \mathrm{e}^{2\lambda s}\tilde{\chi}_1(\xi, s)\,\mathrm{d}s \\ &= 2q^{-\frac{1}{4}}(\xi)\mathrm{e}^{-\lambda\xi}\left(\int_{\tilde{C}_1} + \int_{\tilde{C}_2} + \int_{\tilde{C}_3}\right)\mathrm{e}^{2\lambda s}\tilde{\chi}_1(\xi, s)\,\mathrm{d}s \qquad (5.1)\end{aligned}$$

where $\xi = \int_{x_1}^{x} q^{\frac{1}{2}}\mathrm{d}y$. It should be noted that each term of the sum in (5.1) is a solution to the Schrödinger equation (2.1) (see, for example, [3]). It is also not difficult to see that each of the solutions generated by the integrations along $\tilde{C}_1$ and $\tilde{C}_2$ is proportional to the fundamental solution defined in the sector S_2 of figure 2, whilst the remaining third solution generated by the integration along $\tilde{C}_3$—to $\psi_3(\xi, \lambda)$—is the fundamental solution defined in the sector S_3. (An easy way to establish these facts is to investigate the behaviour of these solutions when ξ goes to ∞_2 and ∞_3 correspondingly (∞_k being the infinity point in sector k).) In this way a linear combination of the fundamental solutions ψ_2 and ψ_3 to form the solution $\psi_1(\xi, \lambda)$ is realized simply by moving the contour $\tilde{C}$ in the s-plane.

The connection problem arises when $\psi_1(\xi, \lambda)$ is continued to sector S_3 by crossing sector S_2, i.e. along some noncanonical path γ_1'' in figure 2. At the end of such a continuation the dominant character of the JWKB factor $q^{-1/4}\exp(-\lambda\xi)$ is lost in favour of the amplitude factor $\chi_1(\xi, \lambda)$ but the series (2.3) does not then give an easy answer to what actually happens when $\mathrm{Re}\,\xi \to \infty$ along such a path. (In fact $\chi_1(\xi, \lambda)$ then behaves as $\exp(2\lambda\xi)$.)

In the s-plane the analytic continuation just described results in a deformation of the contour $\tilde{C}$ to the form shown in figure 16(*d*) (dashed curve). It follows obviously from the figure that the dominant contribution to $\psi_1(\xi, \lambda)$ now comes from the integration along $\tilde{C}_2$, i.e. from the solution proportional to $\psi_2(\xi, \lambda)$, and this is the way by which the connection problem is solved within the framework of the Balian–Bloch representation. (Note that both the solutions defined by the integrations along $\tilde{C}_1$ and $\tilde{C}_3$ are subdominant when $\lambda \to \infty$ and ξ stays in the sector S_3 or when $\mathrm{Re}\,\xi \to \infty_3$ and λ is fixed.)

It is easy to see, further, that the linear combination in the rhs of (5.1) can be explicitly reconstructed with the aid of the canonical coefficients $\alpha_{i/j\to k}$ ($\alpha_{i/j\to k} = \lim_{x\to\infty_k} \frac{\psi_i(x)}{\psi_j(x)}$, see [2]) as follows:

$$\begin{aligned}\psi_1(\xi, \lambda) &= \alpha_{1/2\to p}\psi_2(\xi, \lambda) + \alpha_{1/p\to 2}\psi_p(\xi, \lambda)\\ &= \alpha_{1/2\to p}\psi_2(\xi, \lambda) + \alpha_{1/p\to 2}\alpha_{p/2\to 3}\psi_2(\xi, \lambda) + \alpha_{1/p\to 2}\alpha_{p/3\to 2}\psi_3(\xi, \lambda) \qquad (5.2)\end{aligned}$$

where $p = n + 2$ and where the sequence of terms of the last sum in (5.2) corresponds strictly to the sequence of integrations along $\tilde{C}_1$, $\tilde{C}_2$ and $\tilde{C}_3$ in (5.1). The first linear combination appears in (5.2) when the contour $\tilde{C}_1$ is deformed to the position $\tilde{C}_p$ shown in figure16(*b*).

It is also worthwhile to note that the formula (5.2) giving us the continuation of $\psi_1(\xi, \lambda)$ to sector S_3 along the noncanonical path γ_1'' can be also used to obtain in a simple way the improved connection formula of Silverstone [22] (see also the recent work of Fröman and Fröman [29]) with ψ_3 playing the role of the subdominant contribution. It is enough to this end to substitute each term in the sums in (5.2) by its corresponding JWKB approximation (i.e. none of the cumbersome Borel resummation used by Silverstone is necessary).

6. Exponential asymptotics

The problem of the semiclassical expansions for physical quantities is strictly related to the problem of so-called exponentially small contributions absent (by definition) when only the bare semiclassical expansions of these quantities are considered [23,25–28]. The exponentially small contributions become important if the accuracy of the best semiclassical approximation is considered to be insufficient. There are, however, two aspects of this problem which, according to our knowledge, have not been discussed properly.

The first arises when the corresponding semiclassical series if Borel summed does not correctly reproduce the quantity considered even if it is known that the latter *is* Borel summable. This can happen if the integration path in the Borel plane has been chosen incorrectly.

In fact, there are many such non-homotopic paths in the Borel plane along which a given semiclassical series can be summed. Examples of such different path resummations were given in the previous section (see also [3] for the corresponding discussion). Discrepancies between results of any two of such different path Borel resummations have to be, of course, exponentially small, not contributing to the same semiclassical limit.

In such a case of an incorrectly chosen path, it is enough to find the correct one to reproduce the considered quantity completely, i.e. the corresponding Borel integral then includes *all* the exponentially small contributions.

The second aspect appears when the conditions of the first one are satisfied, i.e. when the Borel transform reproduces *completely* the quantity considered and the semiclassical series is

then used as a source of the best approximation to the Borel integral. As is well known (see, for example, [30]), the latter approximation is obtained in this case by abbreviating the series on its least term (since the series is divergent), the order of which is proportional to the actual value of $\lambda(\overline{h}^{-1})$ (in fact n should be equal to the integer part of $\lambda|s_0|$ where s_0 is a singularity of the Borel function closest to the origin). The remainder (i.e. the difference between the Borel integral and its approximation) is then an exponentially small quantity.

To improve this approximation still using the semiclassical tools, we have to be able to identify the exponential factor of the remainder and to multiply the last factor again by some optimal abbreviation of a new semiclassical expansion of the remainder. Next, we should be able to repeat this procedure to the remainder of the remainder, constructing in this way a more and more accurate semiclassical approximation which includes as many exponentially small contributions as we need to make the approximation as good as we wish. One way to solve this problem has been proposed by Berry and Howls [23] and in a more systematic way by Daalhuis [24]. Our solution to the above problem is formulated in appendix D. According to the beginning of this discussion the exponentially small contributions obtained in this way should be determined by the singularity structure of the corresponding Borel functions, provided, for example, by the topological expansions. In appendix D we show how to get these results.

7. Exponential asymptotics of energy levels

Using the approximation scheme which follows obviously from the topological expansion and from the results of appendix D we shall determine in this section the way of obtaining the semiclassical exponential asymptotic for energy levels of the anharmonic osciallator corresponding to the potential $V(x) = x^2 + x^4$ with the Stokes graph shown in figure 17 and drawn for $E > 0$. Taking into account the symmetry of the potential we can write the quantization condition for the energy levels in the form

$$\exp\left(\frac{\lambda}{2}\oint_K \sqrt{V(x) - E^{\pm}(\lambda)}\,\mathrm{d}x \pm \mathrm{i}\frac{\pi}{2}\right) = \chi_{1\to 3}(E^{\pm}(\lambda), \lambda) \tag{7.1}$$

where the contour K is shown in figure 17 and $\pm$ in (7.1) correspond to the even and odd parities of the levels respectively. (The condition (7.1) is obtained by noting that the fundamental solution $\Psi_4(x, E, \lambda)$ can be *defined* as $\Psi_4(x, E, \lambda) = \pm\mathrm{i}\Psi_1(-x, E, \lambda)$, $x \in S_4$, $\mathrm{Im}\, x = \pm|\mathrm{Im}\, x|$, (the factor $\pm$ ensures that $\Psi_4(x, E, \lambda)$ is real for real x) and that $\Psi_4(x, E, \lambda) = \Psi_1(x, E, \lambda)$ is then a quantization condition for energy levels. If we next continue the latter equation to the infinity of the sector S_3 we get (7.1).)

Making the complex conjugation of both the sides of (7.1) we get an alternative condition for the energy level quantization. Both versions are important since they determine the normal sector of $E(\lambda)$ to be $0 < |\arg\lambda| < 3\pi/2$ for λ sufficiently large [2]. Because of this the semiclassical series of $E(\lambda)$ is, as we have shown in our earlier paper [2] (see also [5–8, 23]), Borel summable to $E(\lambda)$ itself and the singularity structure of $\tilde{E}(s)$ on its Borel plane is also determined by (7.1) and its complex conjugation. It follows from (7.1) that this structure is symmetric with respect to the real axis of the s-plane and $E(\lambda)$ can be recovered by integrating $\tilde{E}(s)$ along the negative half-axis. Of course, to apply to the last integral the procedure of appendix D we have to know a detailed distribution of singularities of $\tilde{E}(s)$ on its Borel plane. But instead of this we can use (7.1) directly to establish the respective exponentially small contributions to $E(\lambda)$. Ordering these contributions according to their exponential smallness we can treat each such contribution as a correction to its predecessors and use the Taylor series expansion to take into account the corresponding contribution. So we can write

$$E(\lambda) = E_0(\lambda) + E_1(\lambda)\ldots \tag{7.2}$$

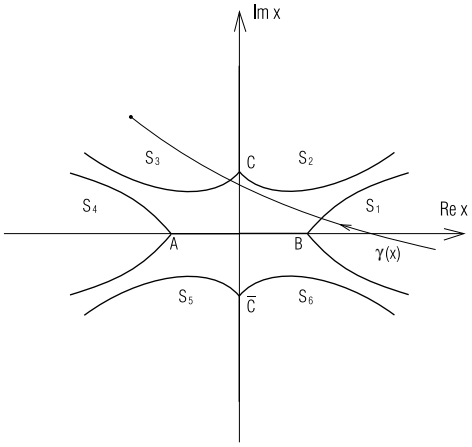

Figure 17. The Stokes graph for the harmonic potential $V(x) = x^2 + x^4$ for $E > 0$.

where $E_0(\lambda)$ is constructed in the standard way, being given as a finite sum arising by the abbreviation at its least term the corresponding semiclassical series for $E(\lambda)$ (see [11]) and, therefore, being polynomially dependent on λ^{-1} whilst further contributions $E_1(\lambda), E_2(\lambda), \ldots,$ in (7.2) are each exponentially smaller than their predecessors.

Of course, $E_0(\lambda)$ for a given λ, has some well defined numerical value around which the corresponding Taylor series expansion of $\chi_{1\to3}(E(\lambda), \lambda)$ can be performed. Thus, we have

$$\chi_{1\to3}(E(\lambda), \lambda) = \chi_{1\to3}(E_0(\lambda), \lambda) + \frac{\partial \chi_{1\to3}(E_0(\lambda), \lambda)}{\partial E}(E_1(\lambda) + E_2(\lambda) + \cdots) + \cdots. \tag{7.3}$$

Since the quantities in (7.2) are real we write the corresponding quantization condition in its real form, too, to get

$$\sin\left(\frac{\lambda}{2\mathrm{i}}\oint_K \sqrt{V(x) - E_0^{\pm}(\lambda)}\,\mathrm{d}x - \frac{\lambda}{4\mathrm{i}}(E_1^{\pm}(\lambda) + E_2^{\pm}(\lambda) + \cdots)\oint_K \frac{\mathrm{d}x}{\sqrt{V(x) - E_0^{\pm}(\lambda)}} + \cdots\right)$$
$$= \mp \mathrm{Re}\left(\chi_{1\to3}(E^{\pm}(\lambda), \lambda) + (E_1^{\pm}(\lambda) + E_2^{\pm}(\lambda) + \cdots)\right.$$
$$\left.\times \frac{\partial \chi_{1\to3}(E_0^{\pm}(\lambda), \lambda)}{\partial E} + \cdots\right). \tag{7.4}$$

It is now clear that we can apply to the coefficient $\chi_{1\to3}(E_0(\lambda), \lambda)$ and its derivatives the procedure of appendix D considering $E_0(\lambda)$ as having well defined value so that the singularity structure of the corresponding Borel function $\tilde{\chi}_{1\to3}(E, s)$ is determined just by the value of E equal to $E_0(\lambda)$.

Assuming the exponential asymptotics for $\chi_{1\to3}(E_0(\lambda), \lambda)$ to be ordered in a way analogous to (7.2), we get for the first two terms of (7.2)

$$\sin\left(\frac{\lambda}{2\mathrm{i}}\oint_K \sqrt{V(x) - E_0^{\pm}(\lambda)}\,\mathrm{d}x\right) = \mp \mathrm{Re}\,(\chi_{1\to3}^{(0)}(E_0^{\pm}(\lambda), \lambda)) \tag{7.5}$$

and

$$E_1^{\pm}(\lambda) = \frac{\pm \mathrm{Re}\,(\chi_{1\to3}^{(1)}(E_0^{\pm}(\lambda), \lambda))}{\frac{\lambda}{4\mathrm{i}}\oint_K \frac{\mathrm{d}x}{\sqrt{V(x) - E_0^{\pm}(\lambda)}} \cos(\frac{\lambda}{2\mathrm{i}}\oint_K \sqrt{V(x) - E_0^{\pm}(\lambda)}\,\mathrm{d}x) \mp \mathrm{Re}\,(\frac{\partial \chi_{1\to3}^{(0)}(E_0^{\pm}(\lambda), \lambda)}{\partial E})} \tag{7.6}$$

where $\chi_{1\to3}^{(0)}(E_0(\lambda), \lambda)$ (we shall suppress the parity indices as unimportant for our further considerations) is given by the respective number of the first terms of the series (2.5) (i.e.

abbreviated at its corresponding least term; note also that the integrations in (2.5) go from ∞_1 to ∞_3 along the canonical path) whilst the exponential contribution $\chi^{(1)}_{1\to3}(E_0(\lambda),\lambda)$ is determined according to appendix D by the singularities of $\tilde{\chi}_{1\to3}(E_0(\lambda),s)$ in its Borel plane closest to the origin.

Applying the approximations following from the topological expansion (A.11) for $\tilde{\chi}_{1\to3}(E_0(\lambda),s)$ we can write (keeping only the first two terms of this expansion)

$$\tilde{\chi}_{1\to3}(E_0(\lambda),s)=\tilde{\Phi}^{(0)}_{1\to3}(E_0(\lambda),s)+\tilde{\Phi}^{(2)}_{1\to3}(E_0(\lambda),s) \tag{7.7}$$

where

$$\begin{aligned}
&\tilde{\Phi}^{(0)}_{1\to3}(E_0(\lambda),s)=I_0\left(\sqrt{4s\int_{\infty_1}^{\infty_3}\tilde{\omega}(\xi,E_0(\lambda))\,\mathrm{d}\xi}\right)\\
&\tilde{\Phi}^{(2)}_{1\to3}(E_0(\lambda,s))=\int_s^0\mathrm{d}\eta\int_{\infty_1}^{\infty_3}\mathrm{d}\xi\tilde{\omega}(\xi+\eta,E_0(\lambda))\tilde{\omega}(\xi,E_0(\lambda))\frac{I_2(\sqrt{z})}{z} \qquad (7.8)\\
&z=4(s-\eta)\int_{\infty_1}^{\infty_3}\tilde{\omega}(\zeta,E_0(\lambda))\,\mathrm{d}\zeta+8(s-\eta)\left(\int_{\infty_1}^{\xi}-\int_{\infty_1}^{\xi+\eta}\right)\tilde{\omega}(\zeta,E_0(\lambda))\,\mathrm{d}\zeta.
\end{aligned}$$

Assuming the same order of approximation for $\chi_1(x,E_0(\lambda),\lambda)$ we can see that when x stays in sector S_3 as shown in figure 18(*a*) then its Borel plane looks as in figure 18(*b*) in which C_1 is the path of the Borel integration to recover $\chi_1(x,E_0(\lambda),\lambda)$. The distribution of the singularities on the figure now follows from (7.7). Figure 18(*c*) shows the Borel plane for $\tilde{\chi}_{1\to3}(E_0(\lambda),s)$, i.e. when $x\to\infty_3$. The singular points are $\zeta_C=\int_{B(E_0(\lambda))}^{C(E_0(\lambda))}\sqrt{V(x)-E_0(\lambda)}\,\mathrm{d}x$, $-\zeta_C$, $\zeta_C-\zeta_A=\int_{A(E_0(\lambda))}^{C(E_0(\lambda))}\sqrt{V(x)-E_0(\lambda)}\,\mathrm{d}x$ and $\zeta_A-\zeta_C$. Therefore, $\chi_{1\to3}(E_0(\lambda),\lambda)$ can be given as

$$\chi_{1\to3}(E_0(\lambda),\lambda)=2\lambda\int_C\mathrm{e}^{2\lambda s}\tilde{\chi}_{1\to3}(E_0(\lambda),s)\,\mathrm{d}s \tag{7.9}$$

where the integration path C is as shown in figure 18(*c*).

The path C differs from the one considered in appendix D but this does not prevent us applying the procedure of this appendix. Therefore, according to the approximation (7.7) we have

$$\chi_{1\to3}(E_0(\lambda),\lambda)=2\lambda\int_C\mathrm{e}^{2\lambda s}(\tilde{\Phi}^{(0)}_{1\to3}(E_0(\lambda),s)+\tilde{\Phi}^{(2)}_{1\to3}(E_0(\lambda),s))\,\mathrm{d}s \tag{7.10}$$

so that

$$\chi^{(0)}_{1\to3}(E_0(\lambda),\lambda)=\sum_{k=0}^{n_0}\frac{(-1)^k}{(2\lambda)^k}\frac{\partial^k}{\partial s^k}(\tilde{\Phi}^{(0)}_{1\to3}(E_0(\lambda),s)+\tilde{\Phi}^{(2)}_{1\to3}(E_0(\lambda),s))|_{s=0} \tag{7.11}$$

where $n_0=[|\lambda\zeta_C|]$.

Using (D.5) and (D.6) of appendix D for $\chi^{(1)}_{1\to3}(E_0(\lambda),\lambda)$ we get

$$\chi^{(0)}_{1\to3}(E_0(\lambda),\lambda)-\sum_{j=C,-C,A-C,C-A}\frac{(n_0+1)!}{(2\lambda)^{n_0}\zeta^{n_0}}\sum_{m=0}^{n_1}\frac{(-1)^m\kappa_j^{(m)}(E_0(\lambda),0)}{(2\lambda)^{m+1}} \tag{7.12}$$

where $\zeta_{-C}=-\zeta_C$, $\zeta_{A-C}=\zeta_A-\zeta_C$, $\zeta_{C-A}=\zeta_C-\zeta_A$, $n_1=[|\lambda\zeta_A|]$ (with $|\zeta_A|$ determining the common distance of singularities of $\kappa_j(E_0(\lambda),s)$ closest to the origin) and κ_j are given by

$$\begin{aligned}
\kappa_j(E_0(\lambda),s)=&\frac{1}{2\pi\mathrm{i}}\int_{K_j}\mathrm{d}t\frac{\tilde{\Phi}^{(2)}_{1\to3}(E_0(\lambda),\zeta_j+t)}{(1+\frac{t}{\zeta_j})^{n_0}}\\
&\times\frac{1}{(t+\zeta_j+\frac{n_0}{\lambda}\ln(1+\frac{t}{\zeta_j})-s)(t+\zeta_j+\frac{n_0}{\lambda}+\frac{n_0}{\lambda}\ln(1+\frac{t}{\zeta_j})-s)}
\end{aligned} \tag{7.13}$$

where the contours K_j surround the cuts originated by the singularities of $\tilde{\Phi}^{(2)}_{1\to3}(E_0(\lambda),s)$ at ζ_j, each shifted to the origin $s=0$ of the Borel plane.

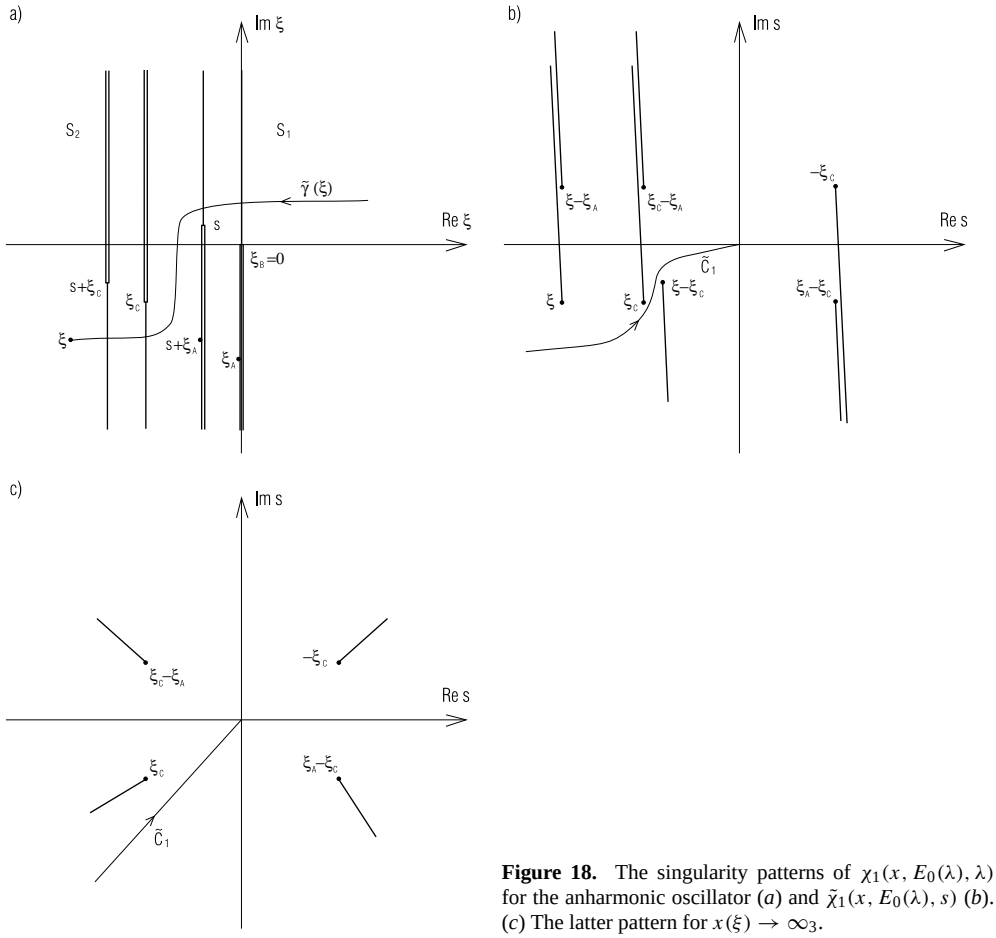

Figure 18. The singularity patterns of $\chi_1(x, E_0(\lambda), \lambda)$ for the anharmonic oscillator (*a*) and $\tilde{\chi}_1(x, E_0(\lambda), s)$ (*b*). (*c*) The latter pattern for $x(\xi) \to \infty_3$.

8. Summary

In this paper we have found the representation for the Borel functions of the quantities relevant for 1D quantum mechanics. The representation takes the form of the topological expansion. This expansion provides us with an algorithm determining in a systematic way the singularity structure of the Borel plane for the relevant quantities and orders the appearing of the Borel plane singularity structures in a hierarchical way allowing for a formulation of the approximation scheme of the semiclassical calculations alternative to others [8–12].

We have also noted the limitations of our method in the description of the proper nature of singularities of the quantities represented by the expansion.

We have formulated the scheme of the semiclassical approximations including the exponentially small contributions to the desired order of accuracy. It makes use of the Borel plane singularity structure in the most natural and effective way, particularly if it is accompanied by the topological expansion method of approximations of the Borel functions.

We have demonstrated the action of both the methods, considering some simple (but not quite trivial) examples of their applications in sections 4, 5 and 7. However, it was not our aim in this paper to perform some numerical tests of the method presented. Rather we have limited ourselves to testing both the methods as theoretical tools for a better understanding of

the mutual relations between the semiclassical expansions, Borel plane singularity structure and the exponential asymptotics. For the latter goal both the expansions (i.e. the topological and the exponential ones) appeared to be very useful. Nevertheless, their test as a practical method of extended semiclassical approximations is certainly desired.

Acknowledgments

The idea of this paper originated during my participation in the workshop on exponential asymptotics organized by the Isaac Newton Institute for Mathematical Sciences (Cambridge, June 1995). I am greatly indebted to the organizers of the programme, particularly to M V Berry and C J Howls for inviting me to the workshop and for the inspiring atmosphere of the Institute. This work was supported by KBN 2 PO3B 134 16

Appendix A

A.1. The Laplace transforms $\tilde{Y}^{(q)}_{n;r_1,\dots,r_q}(\xi,s)$

We shall determine below the Laplace transforms $\tilde{Y}^{(q)}_{n;r_1,\dots,r_q}(\xi,s)$, $n \geqslant q \geqslant 0$, as defined by (3.5). To begin with consider first the case $r_1 = 0$ and $q = 1$. We have

$$\begin{aligned} &Y^{(1)}_{n;r}(\xi,\lambda) = \int_{\tilde{\gamma}_1(\xi)} \mathrm{d}\xi_1 \dots \int_{\tilde{\gamma}_1(\xi_{n-1})} \mathrm{d}\xi_n \tilde{\omega}(\xi_1)\dots\tilde{\omega}(\xi_r)\dots\tilde{\omega}(\xi_n)\mathrm{e}^{2\lambda(\xi-\xi_r)} \\ &r = 1,\dots,n \qquad n = 1,2,\dots. \end{aligned} \tag{A.1}$$

The multiple integral in (A.1) can be rewritten further as follows:

$$\begin{aligned} &Y^{(1)}_{n;r}(\xi,\lambda) = \int_{\tilde{\gamma}_1(\xi)} \mathrm{d}\xi_r \mathrm{e}^{2\lambda(\xi-\xi_r)}\tilde{\omega}(\xi_r)\Omega_{r-1}(\xi,\xi_r)Y^{(0)}_{n-r;}(\xi_r) \\ &r = 1,\dots,n \qquad n = 1,2,\dots \end{aligned} \tag{A.2}$$

where $Y^{(0)}_{n-r;}(\xi_r)$ is defined by (3.3) and

$$\Omega_{r-1}(\xi,\xi_r) = ((r-1)!)^{-1}(\Omega(\xi)-\Omega(\xi_r))^{r-1}. \tag{A.3}$$

Making in (A.2) a change $\xi_r \to \xi - s$ of the integration variable we get

$$\begin{aligned} &Y^{(1)}_{n;r}(\xi,\lambda) = \int_{\tilde{C}} \mathrm{d}s \mathrm{e}^{2\lambda s}\tilde{Y}^{(1)}_{n;r}(\xi_r) \\ &r = 1,\dots,n \qquad n = 1,2,\dots \end{aligned} \tag{A.4}$$

where

$$\tilde{Y}^{(1)}_{n;r}(\xi,s) = -\tilde{\omega}(\xi-s)\Omega_{r-1}(\xi,\xi-s)Y^{(0)}_{n-r;}(\xi-s) \tag{A.5}$$

and the contour $\tilde{C}$ runs from the infinity $\mathrm{Re}\, s = -\infty$ to the origin $s = 0$. Note that because of $\mathrm{Re}\,\xi > 0$ (by assumption) the contour $\tilde{C}$ is independent of r and n and also, as follows from (A.5), $\tilde{Y}^{(1)}_{n;r}(\xi,s)$ is holomorphic for $\mathrm{Re}\, s < \mathrm{Re}\,\xi$.

Reasoning similarly for $\tilde{Y}^{(2)}_{n;r_1r_2}(\xi,s)$ we get

$$\tilde{Y}^{(2)}_{n;r_1r_2}(\xi,s) = -\int_{\tilde{\gamma}(\xi-s)} \mathrm{d}\xi_1 \tilde{\omega}(\xi_1+s)\tilde{\omega}(\xi_1)\Omega_{r_1-1}(\xi,\xi_1+s)\Omega_{r_2-r_1-1}(\xi_1+s,\xi_1)Y^{(0)}_{n-r_2;}(\xi_1). \tag{A.6}$$

The remaining Laplace transforms $\tilde{Y}^{(2q+1)}_{n;r_1\dots r_{2q+1}}(\xi,s)$ and $\tilde{Y}^{(2q)}_{n;r_1\dots r_{2q}}(\xi,s)$, $q=1,2,\dots$ can be defined recurrently as follows:

$$\begin{aligned}\tilde{Y}^{(2q)}_{n;r_1r_2r_3\dots r_{2q}}(\xi,s) &= -\int_{\tilde{C}(s)} \mathrm{d}\eta \int_{\tilde{\gamma}(\xi-s)} \mathrm{d}\xi_1 \tilde{\omega}(\xi_1+s)\tilde{\omega}(\xi_1+\eta)\Omega_{r_1-1}(\xi,\xi_1+s)\\ &\quad\times\Omega_{r_2-r_1-1}(\xi_1+s,\xi_1+\eta)\tilde{Y}^{(2q-2)}_{n-r_2;r_3-r_2\dots r_{2q}-r_2}(\xi_1+\eta,\eta)\end{aligned} \tag{A.7}$$

$q=2,3,\dots$

and

$$\begin{aligned}\tilde{Y}^{(2q+1)}_{n;r_1r_2r_3\dots r_{2q+1}}(\xi,s) &= -\int_{\tilde{C}(s)} \mathrm{d}\eta\tilde{\omega}(\xi-s+\eta)\Omega_{r_1-1}(\xi,\xi_1-s+\eta)\\ &\quad\times\tilde{Y}^{(2q)}_{n-r_1;r_2-r_1\dots r_{2q+1}-r_1}(\xi_1-s+\eta,\eta) \qquad q=1,2,\dots.\end{aligned} \tag{A.8}$$

All of them are holomorphic in ξ and s for $\operatorname{Re}\xi>0$ and $\operatorname{Re}s<\operatorname{Re}\xi$. The contour $\tilde{C}(s)$ in (A.7), (A.8) starts at the point s with $\operatorname{Re}s<\operatorname{Re}\xi$ and ends at $s=0$.

A.2. Topological expansion

A further step we can do is to fix q and to take sums with respect to $n, r_1,\dots,r_{2q}$. This can be done as follows. First, we consider $\chi_1(\xi,\lambda)/(2\lambda)$ rather than $\chi_1(\xi,\lambda)$ itself. Next we note that to each term $-(-2\lambda)^{-n-1}\tilde{Y}^{(q)}_{n;r_1\dots r_q}(\xi,s)$ there corresponds the following Laplace transform:

$$\frac{1}{n!}s^n * \tilde{Y}^{(q)}_{n;r_1\dots r_q}(\xi,s) \tag{A.9}$$

where the star means the convolution of the factors.

The sums we are now looking for are the following:

$$\tilde{\Phi}^{(q)}_1(\xi,s) = \sum_{1\leqslant r_1<\dots<r_q\leqslant n} \frac{(-1)^{r_1+r_2+\dots+r_q}}{n!}s^n * \tilde{Y}^{(q)}_{n;r_1\dots r_q}(\xi,s) \tag{A.10}$$

so that the series

$$\tilde{\Phi}_1(\xi,s) = \sum_{q\geqslant 0}\tilde{\Phi}^{(q)}_1(\xi,s) \tag{A.11}$$

(its convergence is discussed below) represents a function $\tilde{\Phi}_1(\xi,s)$ such that $\partial\tilde{\Phi}_1(\xi,s)/\partial s$ is the Laplace transform of $\chi_1(\xi,\lambda)$.

The sums in (A.10) can be performed explicitly to give

$$\begin{aligned}&\tilde{\Phi}^{(0)}_1(\xi,s) = I_0\left(\sqrt{4s\Omega(\xi)}\right)\\ &\tilde{\Phi}^{(2q)}_1(\xi,s) = \int_{\tilde{C}(s)}\mathrm{d}\eta_1\int_{\tilde{C}(\eta_1)}\mathrm{d}\eta_2\dots\int_{\tilde{C}(\eta_{q-1})}\mathrm{d}\eta_q\int_\infty^{\xi-\eta_1}\mathrm{d}\xi_1\int_\infty^{\xi_1}\mathrm{d}\xi_2\dots\int_\infty^{\xi_{q-1}}\mathrm{d}\xi_q\\ &\qquad\times\tilde{\omega}(\xi_1+\eta_1)\tilde{\omega}(\xi_1+\eta_2)\dots\tilde{\omega}(\xi_q+\eta_q)\tilde{\omega}(\xi_q)(2s-2\eta_1)^{2q}\frac{I_{2q}(z_{2q}^{\frac{1}{2}})}{z_{2q}^q}\\ &z_{2q} = 4(s-\eta_1)\Omega(\xi)+8(s-\eta_1)\sum_{p=1}^{q}(\Omega(\xi_p+\eta_{p+1})-\Omega(\xi_q+\eta_p))\\ &\eta_{q+1}\equiv 0 \qquad q=1,2,\dots\\ &\tilde{\Phi}^{(2q+1)}_1(\xi,s) = \int_{\tilde{C}(s)}\mathrm{d}\eta_1\dots\int_{\tilde{C}(\eta_q)}\mathrm{d}\eta_{q+1}\tilde{\omega}(\xi-\eta_1+\eta_2)\int_\infty^{\xi-\eta_1}\mathrm{d}\xi_1\dots\int_\infty^{\xi_{q-1}}\mathrm{d}\xi_q\end{aligned} \tag{A.12}$$

$$\times\tilde{\omega}(\xi_1+\eta_2)\tilde{\omega}(\xi_1+\eta_3)\ldots\tilde{\omega}(\xi_q+\eta_{q+1})$$
$$\times\tilde{\omega}(\xi_q)(2s-2\eta_1)^{2q+1}\frac{I_{2q+1}(z_{2q+1}^{\frac{1}{2}})}{z_{2q+1}^{\frac{2q+1}{2}}}$$

$$z_{2q+1}=4(s-\eta_1)\Omega(\xi)+8(s-\eta_1)\sum_{p=0}^{q}(\Omega(\xi_p+\eta_{p+2})-\Omega(\xi_p+\eta_{p+1}))$$

$$\xi_0\equiv\xi\qquad\eta_{q+2}\equiv 0\qquad q=0,1,2,\ldots.$$

The functions $I_q(x)$, $q\geqslant 0$, in (A.12) are modified Bessel functions (of the first kind, see [32] p 5, formula (12)). The results (A.12) have been obtained from (A.10) by repeatedly using the following sum rule [32]:

$$\sum_{k\geqslant 0}\frac{1}{k!}\left(\frac{t}{2}\right)^k z^{-\frac{\nu+k}{2}}I_{\nu+k}(z^{\frac{1}{2}})=(z+t)^{-\frac{\nu}{2}}I_\nu((z+t)^{\frac{1}{2}}) \tag{A.13}$$

valid for any ν.

Formulae (A.12) provide us with the general forms of $\tilde{\Phi}_1^{(q)}(\xi,s)$. However, for the singularity analysis of the latter the more convenient representation for them is the following recurrent one:

$$\begin{aligned}\tilde{\Phi}_1^{(2q+2)}(\xi,s)&=-\int_{\tilde{C}(s)}\mathrm{d}\eta\int_{\tilde{C}(\eta)}\mathrm{d}\eta'\int_{\tilde{\gamma}(\eta)}\mathrm{d}\eta_1\tilde{\omega}(\xi_1)\tilde{\omega}(\xi_1-\eta')(2s-2\eta)\\&\quad\times\tilde{\Phi}_1^{(2q)}(\xi_1-\eta',\eta-\eta')\frac{I_1(\sqrt{4(s-\eta)(\Omega(\xi)-2\Omega(\xi_1)+\Omega(\xi_1-\eta'))})}{\sqrt{4(s-\eta)(\Omega(\xi)-2\Omega(\xi_1)+\Omega(\xi_1-\eta'))}}\\\tilde{\Phi}_1^{(2q+1)}(\xi,s)&=-\int_{\tilde{C}(s)}\mathrm{d}\eta\int_{\tilde{C}(\eta)}\mathrm{d}\eta'\tilde{\omega}(\xi-\eta')\\&\quad\times\tilde{\Phi}_1^{(2q)}(\xi-\eta',\eta-\eta')I_0\left(\sqrt{-4(s-\eta)(\Omega(\xi)-\Omega(\xi-\eta'))}\right)\end{aligned} \tag{A.14}$$

$q=0,1,2,\ldots$

where $\tilde{\Phi}_1^{(0)}(\xi,s)$ is given by (A.12).

Note that (A.14) can be obtained from (A.12) and vice versa by applying the following relations:

$$\begin{aligned}\int_0^1\mathrm{d}x\,I_m(\sqrt{\alpha x})I_m\left(\sqrt{\beta(1-x)}\right)(\alpha x)^{\frac{1}{2}m}(\beta(1-x))^{\frac{1}{2}n}&=2\alpha^m\beta^n\frac{I_{m+n+1}(\sqrt{\alpha+\beta})}{(\sqrt{\alpha+\beta})^{m+n+1}}\\\times\frac{(s-\eta)^n}{n!}&=\frac{1}{(k-1)!(n-k)!}\int_\eta^s\mathrm{d}\eta'(s-\eta')^{k-1}(\eta'-\eta)^{n-k}.\end{aligned} \tag{A.15}$$

A.3. Analytic properties of the functions $\tilde{\Phi}_1^{(q)}(\xi,s)$

Since each of the functions $I_q(z_q^{1/2})/z_q^{q/2}$, $q\geqslant 0$, is an entire function of its argument then it follows from (A.12) that possible singularities of $\tilde{\Phi}_1^{(q)}(\xi,s)$ are generated by the (known) singularities of the functions $\tilde{\omega}(\eta)$ and $\Omega(\eta)$ and their integrations present in (A.12). However, it can be easily checked that the conditions

$$\mathrm{Re}\,\xi>0\qquad\text{and}\qquad\mathrm{Re}\,s<\mathrm{Re}\,\xi \tag{A.16}$$

determine the domain where the integrands in (A.12) are holomorphic. Therefore, this is also the domain of holomorphicity of $\tilde{\Phi}_1^{(q)}(\xi,s)$ since all the integration paths in (A.1), (A.12) can be chosen to lie completely in this domain.

Let us note, however, that as follows from (A.12), each $\tilde{\Phi}_1^{(q)}(\xi, s)$, $q \geqslant 1$ can be continued analytically from the domain (A.16) to any point ξ of the ξ-Riemann surface of $\tilde{\Phi}_1^{(q)}(\xi, s)$ (obtained for fixed s) if the distribution of branch points of $\tilde{\omega}(\xi)$ along a path of the corresponding analytical continuation is such that the distance of any of them from the path is greater than $|s|$. This statement is the direct conclusion from the corresponding formulae in (A.12) since all the integrations on the ξ-Riemann surface present there are performed inside a strip no wider than $|s|$.

Let us note further that for the polynomial potentials the branch points of $\tilde{\omega}(\eta)$ are isolated and on each sheet of the ξ-Riemann surface of $\tilde{\omega}(\eta)$ their numbers are finite. The distances between them on each sheet are nothing but the corresponding distances between turning points measured by the action. Therefore, there is the smallest distance d among them. If we take, therefore, s in (A.12) such that $|s| < d' < d/2$ then we can penetrate by paths of the analytical continuations the whole ξ-Riemann surface of $\tilde{\omega}(\xi)$ if the former is deprived all the circular vicinities of radius d'', $d' < d'' < d/2$, centred at each branch point of the surface. We shall denote the corresponding part of the ξ-Riemann surface as $\boldsymbol{R}(d'')$.

Consider now a question of convergence of the series in (A.11). We shall show below that the series is convergent absolutely and uniformly in the domain $\boldsymbol{R}(d'')$. This means that the series (A.11) determines $\tilde{\Phi}_1(\xi, s)$ as the holomorphic function in these domains.

To this end let us note that if $|s|$ is chosen to satisfy the condition $|s| < d' < d''$ all the integration paths $\tilde{\gamma}(\xi - \eta_1)$ can then be deformed to lie inside an infinite strip $S(\xi, s)$ bounded by the paths $\tilde{\gamma}(\xi)$ and $\tilde{\gamma}(\xi - s)$ so having the width $|s|$ with the one end of the strip being placed at the infinity ∞_1 and the other one being a segment $(\xi, \xi - s)$. The latter bound can be chosen as such because the path $\tilde{C}(s)$ can be deformed to a segment (with its ends anchored at the origin and at s). Introducing now the following functions:

$$\begin{aligned} |\tilde{\omega}|(\xi_r, \eta_1) &= \limsup_{\eta \in \tilde{C}(\eta_1)} |\tilde{\omega}(\xi_r + \eta_1)| \\ |\tilde{\rho}|(\xi, \eta_1) &= \int_{\tilde{\gamma}_1(\xi)} |\mathrm{d}\xi_r||\tilde{\omega}|(\xi_r, \eta) \end{aligned} \tag{A.17}$$

we have

$$|\Omega(\xi_r + \eta)| < \tilde{\rho}(\xi, \eta_1) \qquad \eta \in \tilde{C}(\eta_1) \qquad \xi_r \in \tilde{\gamma}_1(\xi) \tag{A.18}$$

and for q large enough

$$\begin{aligned} |z_q| &< 8(q+1)|s - \eta_1|\tilde{\rho}(\xi, \eta_1) \\ |2^q z_q^{-\frac{q}{2}} I_q| &< \frac{1}{q!} \exp(2|s - \eta_1|\tilde{\rho}(\xi, \eta_1)) \end{aligned} \tag{A.19}$$

so that

$$\begin{aligned} |\tilde{\Phi}_1^{(2q)}(\xi, s)| &< ((2q)!q!(q-1)!)^{-1} \int_0^{|s|} \mathrm{d}x x^{q-1}(|s| - x)^{2q} \\ &\quad \times \left(\int_{\tilde{\gamma}_1(\xi - \eta_1)} |\mathrm{d}\eta||\tilde{\omega}|^2(\eta, \eta_1) \right)^q \exp(2(|s| - x)\tilde{\rho}(\xi, \eta_1)) \\ |\tilde{\Phi}_1^{(2q+1)}(\xi, s)| &< ((2q+1)!(q!)^2)^{-1} \int_0^{|s|} \mathrm{d}x x^q(|s| - x)^{2q+1}|\tilde{\omega}|(\eta, \eta_1) \\ &\quad \times \left(\int_{\tilde{\gamma}_1(\xi - \eta_1)} |\mathrm{d}\eta||\tilde{\omega}|^2(\eta, \eta_1) \right)^q \exp(2(|s| - x)\tilde{\rho}(\xi, \eta_1)) \end{aligned} \tag{A.20}$$

where $x = |\eta_1|$.

Introducing

$$\begin{aligned}|\omega|(\xi,s) &= \limsup_{\eta_1\in\tilde{C}(s)} |\tilde{\omega}|(\xi,\eta_1)\\ \rho(\xi,s) &= \limsup_{\eta_1\in\tilde{C}(s)} \tilde{\rho}(\xi,\eta_1)\\ Q(\xi,s) &= \limsup_{\eta_1\in\tilde{C}(s)} \int_{\tilde{\gamma}_1(\xi-\eta_1)} |\mathrm{d}\eta||\tilde{\omega}|(\eta,\eta_1)\end{aligned} \tag{A.21}$$

we obtain finally for $q\to\infty$

$$\begin{aligned}|\tilde{\Phi}_1^{(2q)}(\xi,s)| &< \frac{|s|^{3q}}{(3q)!q!}Q^{2q}(\xi,s)\mathrm{e}^{2|s|\rho(\xi,s)}\\ |\tilde{\Phi}_1^{(2q+1)}(\xi,s)| &< \frac{|s|^{3q+2}}{(3q+2)!q!}Q^{2q}(\xi,s)|\omega|(\xi,s)\mathrm{e}^{2|s|\rho(\xi,s)}.\end{aligned} \tag{A.22}$$

The bounds (A.22) show clearly that the series (A.11) is convergent in the assumed domain $\boldsymbol{R}(d'')$ since $Q(\xi,s)$, $\rho(\xi,s)$ and $|\omega|(\eta,s)$ are finite there.

Appendix B

If x_p is a simple zero of $q(x)$ then the point $\xi_p=\xi(x_0,x_p)$ is the branch point for the function $\tilde{\omega}(\xi)$ defined by (2.5) which can be expounded around the point ξ_p into the following series:

$$\tilde{\omega}(\xi)=\sum_{k\geqslant -3}\tilde{\omega}_k(\xi_p)(\xi-\xi_p)^{2k/3}. \tag{B.1}$$

The coefficients $\tilde{\omega}_k(\xi_p)$ in (B.1) are defined by the identity $\tilde{\omega}(\xi(x_0,x))\equiv\omega(x)q^{-\frac{1}{2}}(x)$ and the following expansions of $\xi(x_0,x)$ and $\omega(x)q^{-\frac{1}{2}}(x)$ (see (2.4)) around x_p:

$$\begin{aligned}\xi(x_0,x)-\xi_p &= \sum_{k\geqslant 0}\xi_k(x_p)(x-x_p)^{k+\frac{3}{2}}\\ \omega(x)q^{-\frac{1}{2}}(x) &= \sum_{k\geqslant 0}\omega_k(x_p)(x-x_p)^{k-3}.\end{aligned} \tag{B.2}$$

In particular, the coefficient at the most singular term in (B.1) $\tilde{\omega}_{-3}=\frac{-5}{36}$, i.e. it is potential independent. It depends, however, on the multiplicity of zero of $q(x)$ at x_p, namely $\tilde{\omega}_{-3}=-n(n+4)/[4(n+2)^2]$ for the n-fold zero.

Appendix C

We establish here the Riemann surface structure of $\tilde{\Phi}_1^{(q)}(\xi,s)$ for the linear and harmonic potentials.

C.1. The linear potential

According to section 4.1 the Riemann surface structure of $\tilde{\Phi}_1^{(1)}(\xi,s)$ for this case is determined by

$$\tilde{\Phi}_1^{(1)}(\xi,s)=-\frac{5}{8}\int_{\tilde{C}(s)}\mathrm{d}\eta\frac{s-\eta}{(\xi-\eta)^2}\frac{I_1((\frac{5}{2}\frac{s-\eta}{\xi-\eta}-\frac{5}{4}\frac{s-\eta}{\xi})^{\frac{1}{2}})}{(\frac{5}{2}\frac{s-\eta}{\xi-\eta}-\frac{5}{4}\frac{s-\eta}{\xi})^{\frac{1}{2}}}. \tag{C.1}$$

From (C.1) it follows that its subintegral function is singlar at $\xi=\eta$ and at $\xi=0$ where it behaves as $\mathrm{e}^{\pm(\xi-\eta)^{-\frac{1}{2}}}(\xi-\eta)^{-\frac{7}{4}}$ and $\mathrm{e}^{\pm\xi^{-\frac{1}{2}}}\xi^{\frac{1}{2}}$ respectively. The η-integration generates only

a singularity at $s = \xi$ (by the EP mechanism) leaving the singularity at $\xi = 0$ and its character unchanged. Therefore, assuming ξ to be continued to sector S_2 (along the canonical path) the corresponding first sheets of the Riemann surface look as in figures 10(*a*) and (*b*).

Consider now $\tilde{\Phi}_1^{(2)}(\xi, s)$. Its Riemann surface structure is defined by

$$\tilde{\Phi}_1^{(2)}(\xi, s) = -\frac{25}{64}\int_{\tilde{C}(s)} \mathrm{d}\eta \int_{\tilde{\gamma}(\xi)} \mathrm{d}\xi_1 \frac{(s-\eta)^2}{(\xi-\eta)^2\xi_1^2}\frac{I_2(z^{\frac{1}{2}})}{z}$$
$$z = \frac{5}{4}(s-\eta)\left(\frac{1}{\xi} - \frac{2}{\xi_1} + \frac{2}{\xi_1 - \eta}\right). \tag{C.2}$$

It follows from (C.2) that the subintegral function is singular at $\xi_1 = \eta$, $\xi = 0$ and at $\xi_1 = 0$ behaving there as $\mathrm{e}^{\pm(\xi_1-\eta)^{-\frac{1}{2}}}(\xi_1-\eta)^{-\frac{7}{4}}$, $\mathrm{e}^{\pm\xi^{-\frac{1}{2}}}\xi^{\frac{1}{2}}$ and $\mathrm{e}^{\pm\xi_1^{-\frac{1}{2}}}\xi_1^{-\frac{7}{4}}$ respectively.

The ξ_1-integration in (C.2) generates the EP singularities at $\xi = \eta$ and at $\xi = 0$ but also the P singularity at $\eta = 0$ (when the singularity at $\xi_1 = \eta$ move around the endpoint of $\tilde{\gamma}(\xi)$ clockwise, pinching the latter against the singular point $\xi_1 = 0$).

The final η-integration in (C.2) generates the EP singularity at $s = \xi$ and $s = 0$ and the P singularity at $\xi = 0$. Therefore, the 'closest' singularities of $\tilde{\Phi}_1^{(2)}(\xi, s)$ are the following:

$$\xi = 0 \qquad \xi = \eta \qquad s = 0. \tag{C.3}$$

Let us make a general note that the EP mechanism repeats the distribution of the branch points and cuts whilst the P one generates new branch points on the Riemann surfaces obtained by the EP mechanism always however enforcing specific ways of moving around the singularities generated by the EP mechanism.

All the singularities in (C.3) are the root branch points (of the fourth order) accompanied by essential singularities as we have mentioned above. The singularity at $s = 0$, however, to be reached needs to round the branch point at $s = \xi$ moving clockwise, i.e. it lies on the sheet opened by the latter branch point. This singularity is therefore a consequence of the singularity at $\xi = 0$.

A similar note concerns the singularity at $\xi = 0$. In fact there are two such singularities the one on the sheet shown in figure 10(*a*) (arising by the EP mechanism) and the second one at the sheet opened by the branch point at $\xi = \eta$, i.e. to reach it one needs to round this point clockwise.

One can conclude therefore that the P mechanism applied once has generated a singularity at $s = 0$ and applied twice has generated a new singularity at $\xi = 0$ (on a different sheet) from the old one. It is clear that this mechanism will proliferate the last singularity on all the sheets of the Riemann surface of $\tilde{\Phi}_1(\xi, s)$ except the sheet we have started with on which the point $s = 0$ is regular for $\tilde{\Phi}_1(\xi, s)$.

Now we can use the formulae (A.14) to prove the form of the first sheet of the Riemann surface as shown in figures 10(*a*) and (*b*). Namely, assuming for $\tilde{\Phi}_1^{(2q)}(\xi, s)$ the form of this sheet shown in the last figure we deduce that it remains unchanged for $\tilde{\Phi}_1^{(2q+2)}(\xi, s)$ whilst it is deprived of the singularity at $s = 0$ for $\tilde{\Phi}_1^{(2q+1)}(\xi, s)$.

Indeed, consider the subintegral function in the first of the formulae (A.14) defining $\tilde{\Phi}_1^{(2q+2)}(\xi, s)$. It has singularities at the following points:

$$\xi = 0 \qquad \xi_1 = 0 \qquad \xi_1 - \eta' = 0 \qquad \xi_1 - \eta = 0 \qquad \eta - \eta' = 0 \tag{C.4}$$

shown in figure C.1(*a*) for the ξ_1-Riemann surface (when the rest of the variables are fixed).

The ξ_1-integration provides us with the EP singularities at $\xi = 0$, $\xi - \eta = 0$ and $\xi - \eta' = 0$ and with the P ones at $\eta = 0$, $\eta' = 0$ (when the point ξ is rounded by η and η' clockwise to touch the point $\xi = 0$ by the latter) and at $\eta = \eta'$ (when the point $\eta(\eta')$ rounds ξ clockwise

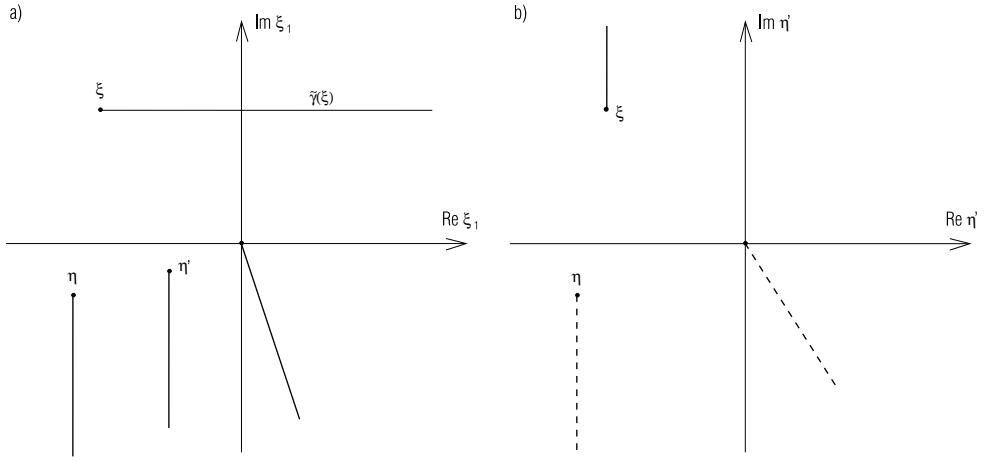

Figure C.1. The 'first sheets' singularity pattern of the subintegral function defining $\tilde{\Phi}_1^{(2q+1)}(\xi, s)$ for the linear potential (*a*) before the ξ_1-integration and (*b*) after it.

(anticlockwise) to touch $\eta'(\eta)$). In this way we get the singularity pattern before the η'-integration shown in figure C.1(*b*) where the singularities at $\eta' = 0$ and at $\eta' = \eta$ are screened by the ξ-cut and to get them one has to go around ξ clockwise or anticlockwise respectively.

The η'-integration therefore does not do much now, providing us with the singularity at $\eta = \xi$ and at $\eta = 0$ (by the EP mechanism) and at $\xi = 0$ (by the P one) with the latter singularity placed on a sheet opened by the singularity at $\xi = \eta$.

The final η-integration only repeats the singularity pattern described above so we are left with the distribution of the singularities as shown in figures 10(*a*) and (*b*).

Consider now the second formula (A.14). There is no the ξ_1-integration and therefore the singularity at $\eta' = 0$ is not generated and the other singularities at $\xi = 0$, $\eta = 0$ and $s = 0$ cannot be generated either by further η'- and η-integrations. Also, the generation of the singularities at $\xi = s$ goes exactly in the same way so that the final picture of the corresponding Rieman surface is the same as in figure 10, apart from missing the respective singularities at $\xi = 0$ and $s = 0$ on the lower sheets.

C.2. The harmonic potential

We assume here $\tilde{\gamma}_1(\xi)$ to be continued canonically to sector S_3 of figure 11 and we put $\xi(i) = \int_{-i}^{i} \sqrt{x^2 + 1}\mathrm{d}x = \zeta$. Neither $\tilde{\omega}(\xi)$ nor $\Omega(\xi)$are now simple functions of ξ. $\tilde{\omega}(\xi)$ is periodic (with its period 2ζ acting between different sheets of the infinitely sheeted Riemann surface on which this function is defined) whilst $\Omega(\xi)$ is not.

Consider again, however, $\tilde{\Phi}_1^{(1)}(\xi, s)$ as given by (4.1). The closest singularities of the subintegral function are shown in figure C.2, i.e. they are

$$\xi = 0 \qquad \xi - \zeta = 0 \qquad \xi - \eta = 0 \qquad \xi - \eta - \zeta = 0. \tag{C.5}$$

Therefore the η-integration in (4.1) provides us with the following singularities of $\tilde{\Phi}_1^{(1)}(\xi, s)$ shown in figure 12:

$$\xi = 0 \qquad \xi - \zeta = 0 \qquad \xi - s = 0 \qquad \xi - \zeta - s = 0 \tag{C.6}$$

i.e. no P singularity is generated.

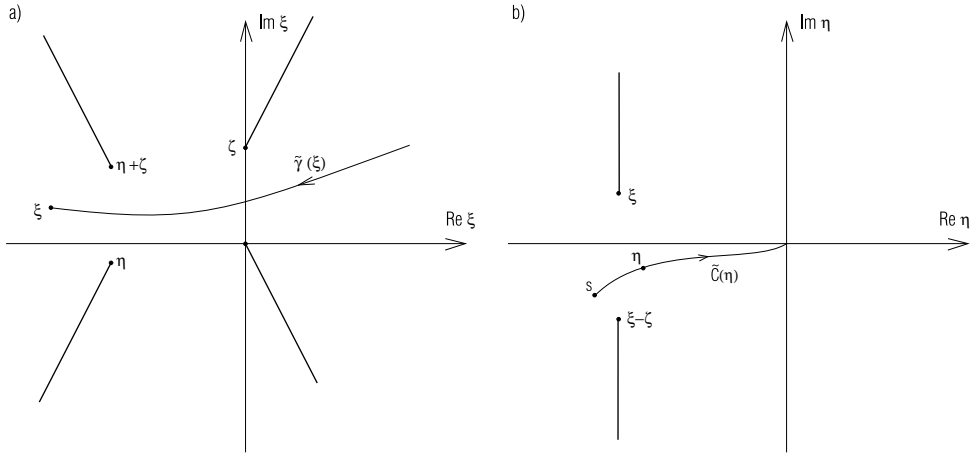

Figure C.2. The singularities of the subintegral function in (4.1) defining $\tilde{\Phi}_1^{(1)}(\xi, s)$ for the harmonic potential.

Consider next $\tilde{\Phi}_1^{(2)}(\xi, s)$. According to (4.3) singularities of the subintegral function in this formula are now

$$\begin{aligned} &\xi = 0 \qquad \xi - \zeta = 0 \qquad \xi_1 = 0 \qquad \xi_1 - \zeta = 0 \\ &\xi_1 - \eta \qquad \xi_1 - \zeta - \eta = 0 \end{aligned} \tag{C.7}$$

and we can use figure C.2 to show the corresponding situation for the ξ_1- and η-dependance by making the substitution $\xi \to \xi_1$ in the figure.

The ξ_1-integration generates the following singularities:

$$\xi = 0 \qquad \xi - \zeta = 0 \qquad \xi - \eta = 0 \qquad \xi - \zeta - \eta = 0 \tag{C.8}$$

by the EP mechanism and

$$\eta = 0 \qquad \eta - \zeta = 0 \qquad \eta + \zeta = 0 \tag{C.9}$$

by the P mechanism. The latter singularities lie on the 'lower' sheets of the η-Riemann surface.

Finally, integrating in (4.3) over η we generate singularities of $\tilde{\Phi}_1^{(2)}(\xi, s)$ at

$$\xi - s = 0 \qquad \xi - \zeta - s = 0 \qquad s - \zeta = 0 \qquad s + \zeta = 0 \tag{C.10}$$

by the EP mechanism and at

$$\xi + \zeta = 0 \qquad \xi = 0 \qquad \xi - \zeta = 0 \qquad \xi - 2\zeta = 0 \tag{C.11}$$

by the P mechanism. The proper distribution of these singularities is shown on figure 13.

Now we can proceed inductively assuming for $\tilde{\Phi}_1^{(2q)}(\xi, s)$ the singularity pattern shown in figure 14 where $\tilde{\gamma}(\xi)$ is the integration path in formulae (A.12)–(A.14) and C the corresponding path to recover from $\chi_1^{(2q)}(\xi, \lambda)$ by the Borel transformation (at $s = 0$ $\tilde{\Phi}_1^{(2q)}(\xi, s)$ is then regular).

Taking into account the second of formulae (A.14) we see that the singularities of the subintegral function are determined mostly by its factor $\tilde{\Phi}_1^{(2q)}(\xi - \eta', \eta - \eta')$ according to which and figure C.3(a) these singularity are at the points

$$\begin{aligned} &\xi - \eta = 0 \qquad \xi - \eta - \zeta = 0 \qquad \xi - \eta' - k\zeta = 0 \qquad k = -(2q-1), \ldots, 2q \\ &\eta' - \eta + k\zeta = 0 \qquad k = -(2q-1), \ldots, (2q-1) \qquad k \neq 0 \end{aligned} \tag{C.12}$$

shown for the case of the corresponding η'-Riemann surface in figure C.3(b).

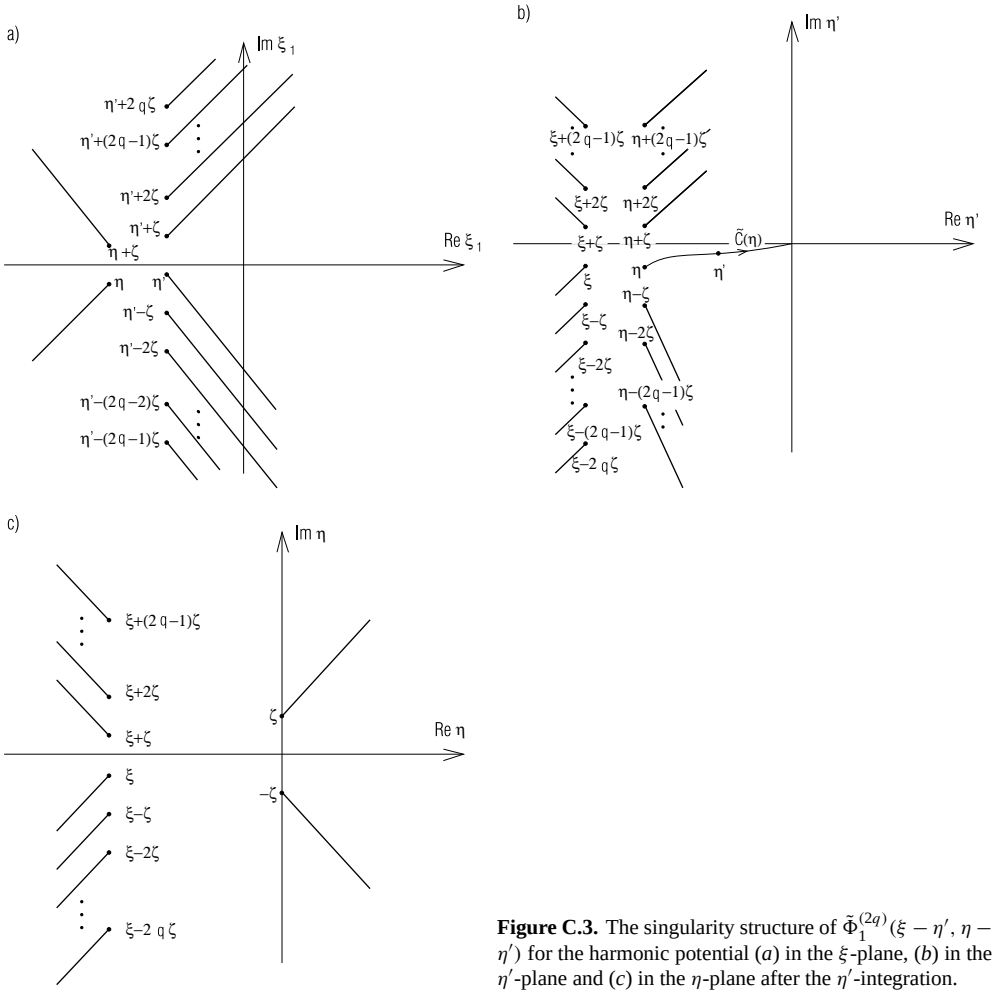

Figure C.3. The singularity structure of $\tilde{\Phi}_1^{(2q)}(\xi-\eta',\eta-\eta')$ for the harmonic potential (*a*) in the ξ-plane, (*b*) in the η'-plane and (*c*) in the η-plane after the η'-integration.

Therefore, making the η'-integration we obtain the 'η-plane' singularity pattern shown in figure C.3(*c*) on which the ξ-dependent singularities are created by the EP mechanism whilst the two fixed ones on the imaginary axis by the P mechanism. Other singularities generated in the last way appear on the lower sheets originated by the two singularities at $\eta=\zeta$ and $\eta=\zeta'$.

The successive η-integration changes nothing in the s-variable singularity pattern (in comparison with this on figure C.3(*c*)) so providing us finally with its form shown in figure 15(*b*), but it seriously changes the original pattern of figure 14(*a*). That is, the EP mechanism generates the ξ-singularities at the points $\xi=s-(2q-1)\zeta, s-(2q-2)\zeta,\ldots,s-\zeta,s,s+\zeta,\ldots,s+2q\zeta$ and by the P-mechanism at the points $\xi=-2q\zeta,\ldots,-\zeta,0,\zeta,\ldots,(2q+1)\zeta$. As the final result we have for $\tilde{\Phi}_1^{(2q+1)}(\xi,s)$ the picture of figure 15 for both types of singularities.

The corresponding analysis of the case $\tilde{\Phi}_1^{(2q+2)}(\xi,s)$ is a little more tedious but nevertheless direct due to the first of the formulae (A.14). The valid singularities of the subintegral function

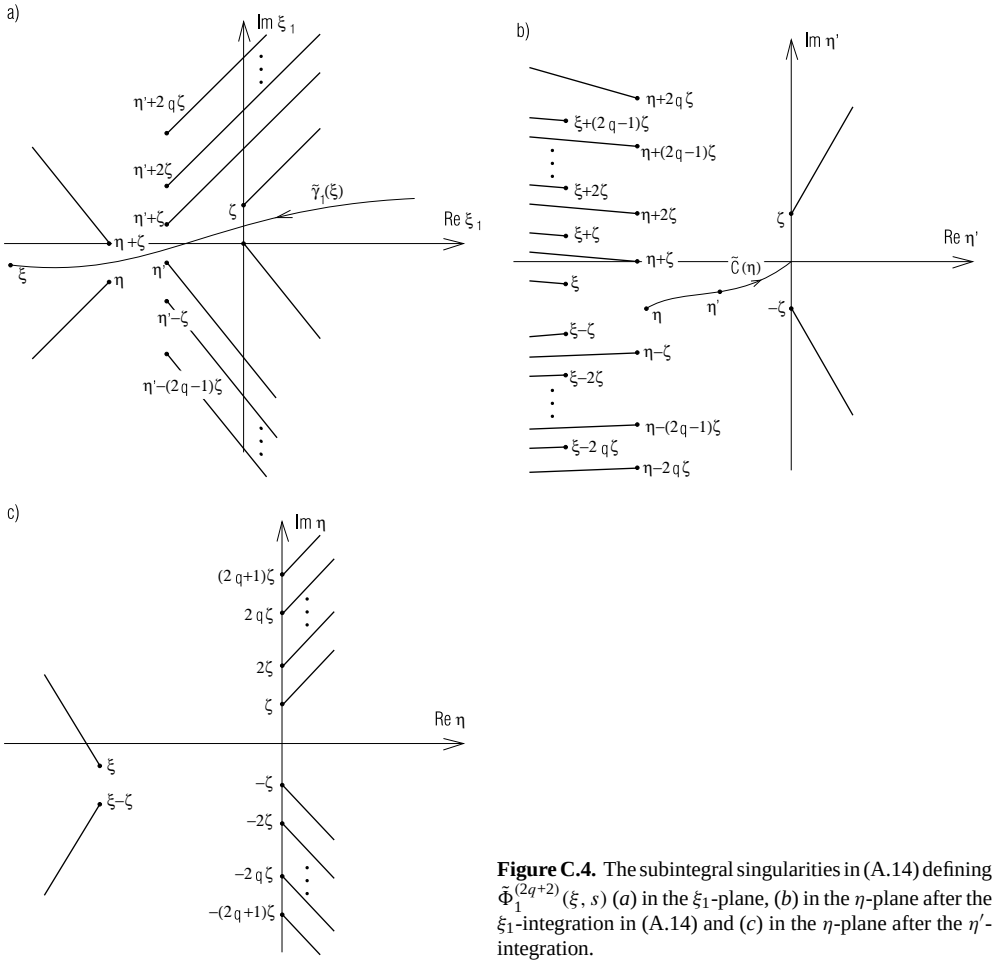

Figure C.4. The subintegral singularities in (A.14) defining $\tilde{\Phi}_1^{(2q+2)}(\xi, s)$ (*a*) in the ξ_1-plane, (*b*) in the η-plane after the ξ_1-integration in (A.14) and (*c*) in the η-plane after the η'-integration.

in this case are

$$\begin{aligned} &\xi_1 = 0 \qquad \xi_1 - \eta = 0 \\ &\xi_1 - \eta = 0 \qquad \xi_1 - \eta - \zeta = 0 \qquad \xi_1 - \eta' - k\zeta = 0 \\ &k = -(2q-1), \ldots, 2q \\ &\eta' - \eta + k\zeta = 0 \qquad k = -(2q-1), \ldots, (2q-1) \qquad k \neq 0. \end{aligned} \tag{C.13}$$

The first ξ_1-integration is performed on the sheet shown in figure C.4(*a*). By the EP and P mechanism it generates η- and η'-singularities. Limiting ourselves to collect only these singularities which appear on the η'-sheet on which the result of this ξ_1-integration is regular at $\eta' = 0$ we arrive at the pattern shown in figure C.4(*b*).

The successive η'-integration leads us to the 'η-plane' pattern shown in figure C.4(*c*) where the two ξ-dependent singularities were produced by the EP mechanism whilst the fixed ones by the EP and P mechanisms simultaneously with the exception of the highest two ones at $\eta = -(2q+1)\zeta$ and $\eta = (2q+1)\zeta$ which are generated by the P mechanism only.

The final η-integration in (A.14) provide us with a pattern analogous to the one of figure 14(*a*) by the EP and P mechanism and with the pattern of figure 14(*b*) by the EP mechanism when q is substituted by $q + 1$.

Appendix D

We describe here a procedure allowing us to construct in a systematic way the optimum semiclassical representation for the Borel summable quantity including both the main contribution coming from the semiclassical series abbreviated at its least term and the corresponding exponential contributions of an arbitrary order. In its finite form the procedure provides us with the exact formula for the quantity considered. However, if continued infinitely the procedure give rise to the question of convergence of the infinite functional series we get by it.

To this goal we shall consider the basic quantity given by the formula (2.8). Integrating in it by parts we get

$$\chi_1(\xi,\lambda)=2\lambda\left(\sum_{k=0}^{n}\frac{(-1)^k}{(2\lambda)^{k+1}}\tilde{\chi}_1^{(k)}(\xi,0)+\frac{(-1)^{n+1}}{(2\lambda)^{n+1}}\int_{\tilde{C}}\mathrm{e}^{2\lambda s}\tilde{\chi}_1^{(n+1)}(\xi,s)\,\mathrm{d}s\right). \tag{D.1}$$

According to the well known prescription (which can be easily justified by the analysis similar to the one performed below) we should put $n=n_0=[\lambda|s_0|]$ in (D.1) where $[x]$ means the integer part of x and s_0 is a singularity of $\tilde{\chi}_1(\xi,s)$ closest to the origin. Next we should extract from the integral the exponentially small factor and finally continue the procedure to the remaining Borel integral. This can be done in the following way.

First the (n_0+1)th derivative of $\tilde{\chi}_1(\xi,s)$ can be given the form

$$\tilde{\chi}_1^{(n_0+1)}(\xi,s)=\frac{(-1)^{n_0+1}(n_0+1)!}{2\pi i}\int_K\tilde{\chi}_1(\xi,s+t)t^{-n_0-2}\,\mathrm{d}t \tag{D.2}$$

with the integration contour K in (D.2) surrounding anticlockwise the negative half-axis of the Borel plane (see figure 5).

As follows from figure 2, $s_0=\xi-\zeta_1=\xi$ (since $\zeta_1=0$, see figure 4). Deforming the contour K to surround the cuts generated by the points $\xi-\zeta_1$ and $\xi-\zeta_2$ of figure 5 (for ξ chosen as in the figure they are the unique cuts visible in these positions) and shifting the integration variable in the corresponding integrals we get

$$\tilde{\chi}_1^{(n+1)}(\xi,s)=\frac{(-1)^{n_0+1}(n_0+1)!}{2\pi\mathrm{i}}\sum_{j=1}^{2}\int_{K_j}\tilde{\chi}_1(\xi-\zeta_j+t)(\xi-\zeta_j-s+t)^{-n_0-2}\,\mathrm{d}t \tag{D.3}$$

where the contours K_j surround (anticlockwise) the cuts whose origins are at the point $t=0$.

Further substituting (D.3) to (D.1) and changing both the order of integrations in (D.3) and the integration variables themselves we get as a result of these calculations

$$\chi_1(\xi,\lambda)=\sum_{k=0}^{n_0}\frac{(-1)^k}{(2\lambda)^k}\tilde{\chi}_1^{(k)}(\xi,0)-\sum_{j=1}^{2}\frac{(n_0+1)!}{(2\lambda)^{n_0}(\xi-\zeta_j)^{n_0}}\int_{\tilde{C}}\mathrm{e}^{2\lambda s}\kappa_j(\xi,s)\,\mathrm{d}s \tag{D.4}$$

where

$$\begin{aligned}\kappa_j(\xi,s)=\frac{1}{2\pi\mathrm{i}}\int_{K_j}\mathrm{d}t\,&\frac{\tilde{\chi}_1(\xi,\xi-\zeta_j+t)}{(1+\frac{t}{\xi-\zeta_j})^{n_0}}\\ &1/\left(t+\xi-\zeta_j+\frac{n_0}{\lambda}\ln\left(1+\frac{t}{\xi-\zeta_j}\right)-s\right)\\ &\times\left(t+\xi-\zeta_j+\frac{n_0}{\lambda}+\frac{n_0}{\lambda}\ln\left(1+\frac{t}{\xi-\zeta_j}\right)-s\right)\end{aligned} \tag{D.5}$$

$j=1,2$

and where the contours K_j run again around the cuts anchored at $t=0$.

The form (D.5) for κ allows us to continue the procedure of getting the asymptotic series expansions for the integrals in (D.4) and to abbreviate the series at their least terms. The latter are to be determind by the singularities generated by the t-integrals in the s-plane (as a result of the pinch mechanism) closest to the origin of the plane. It is easy to see that among possible candidates for the latter are the singularities at $s = \xi$, $\xi + n_0/\lambda$ for $\kappa_1(\xi, s)$ and the ones at $s = \xi - \zeta_2$, $\xi + n_0/\lambda - \zeta_2$ for $\kappa_2(\xi, s)$ (all the singularities are generated by the P mechanism at $t = 0$). However, the integrations in (D.5) along the corresponding cuts open possibilities for new singularities to appear generated by the t-singularities shared by the cuts. These possibilities still enrich the variety of singularities which have to be taken into account in choosing the one closest to the origin of the s-plane.

Therefore, to construct the representation (D.1) for each of the two integrals in (D.4) we have to choose from the singularities corresponding to each κ the ones which are closest to the origin. When these choices are done the procedure described above can be repeated.

Let us call κ_j, $j = 1, 2$, defined by (D.5) the first generation family considering $\kappa_0(\xi, s) \equiv \tilde{\chi}_1(\xi, s)$ as the zeroth generation one. It is clear that the general form of the optimum semiclassical representation for $\chi_1(\xi, \lambda)$ is the following:

$$\begin{aligned}\chi_1(\xi, \lambda) = 2\lambda \sum_{m=0}^{n_0} \frac{(-1)^m \chi_1(\tilde{\xi}, 0)}{(2\lambda)^{m+1}} \\ \times 2\lambda \sum_{k=1}^{p} (-1)^k \sum_{j_1,\ldots,j_k} \prod_{l=1}^{k} \frac{(n_{j_{l-1}} + 1)!}{(2\lambda)^{n_{j_{l-1}}+1} (\xi - \zeta_j)^{n_{j_{l-1}}}} \sum_{m=0}^{n_{j_k}} \frac{(-1)^m \kappa^{(m)}_{j_1,\ldots,j_k}(\xi, 0)}{(2\lambda)^{m+1}} \\ \times 2\lambda (-1)^{p+1} \sum_{j_1,\ldots,j_{p+1}} \prod_{l=1}^{p+1} \frac{(n_{j_{l-1}} + 1)!}{(2\lambda)^{n_{j_{l-1}}+1} (\xi - \zeta_j)^{n_{j_{l-1}}}} \int_{\tilde{C}} \mathrm{e}^{2\lambda s} \kappa_{j_1,\ldots,j_{p+1}}(\xi, s)\, \mathrm{d}s \quad \text{(D.6)}\end{aligned}$$

where $j_0 \equiv 0$ and $\kappa_{j_1 \ldots j_{p+1}}$ constitute the $(p+1)$th generation family. The latter is constructed from the pth one (with ζ_{jp} as its singular points and with $n_{jp}/\lambda = |\zeta^0_{jp}|$ being the singularity closest to the origin) according to the formulae (D.2)–(D.5).

It is important to stress that (D.6) is exact and its rhs becomes an approximation to the left one only when the last sum of the rhs containing the integrals is rejected.

Appendix E

We shall show below that the last term on the rhs sum in (4.15) has to vanish when $\lambda_0 \to 0$. To this end let us note that we can rewrite the integral present in this term in the following way:

$$\begin{aligned}\int_{C'(\lambda_0)} \exp(2\lambda s) \log \chi_{1\to 3}(\lambda)\, \mathrm{d}\lambda = \int_{C_{\frac{1}{2}}} [\exp(2\lambda s) \log \chi_{1\to 3}(\lambda) + \exp(-2\lambda s) \log \chi_{1\to 3}(-\lambda)]\, \mathrm{d}\lambda \\ = \int_{C_{\frac{1}{2}}} [\exp(2\lambda s) - \exp(-2\lambda s)] \log \chi_{1\to 3}(\lambda)\, \mathrm{d}\lambda \\ + \int_{C^d_{\frac{1}{2}}} \exp(-2\lambda s)[1 + \exp(-2\pi \mathrm{i}\lambda)]\, \mathrm{d}\lambda + \int_{C^u_{\frac{1}{2}}} \exp(-2\lambda s)[1 \exp(2\pi \mathrm{i}\lambda)]\, \mathrm{d}\lambda \quad \text{(E.1)}\end{aligned}$$

where $C_{\frac{1}{2}}$ is the half-circle of radius λ_0 lying in the right half of the λ-plane, and $C^u_{\frac{1}{2}}$ and $C^d_{\frac{1}{2}}$ are the corresponding upper and lower halves of $C_{\frac{1}{2}}$. We have also made use of the relations (4.11) to obtain the final form of (C.1). It now follows from (4.10) that we have

$$\lim_{\lambda \to 0} \chi_{1\to 3}(\lambda) = \sqrt{2} \qquad \text{for} \quad |\arg \lambda| < \pi. \quad \text{(E.2)}$$

Therefore, we can conclude that both $\log|\chi_{1\to 3}(\lambda)|$ and $\arg\chi_{1\to 3}(\lambda)$ are bounded in the half-plane $\mathrm{Re}\,\lambda \geqslant 0$. The vanishing of all the integrals in (E.1) when $\lambda_0 \to 0$ now follows directly from the last conclusion.

References

[1] Balian R and Bloch C 1974 *Ann. Phys., NY* **108** 514
[2] Giller S 1992 *Acta Phys. Pol.* B **23** 457–511
[3] Giller S and Milczarski P 1998 Borel summable solutions to Schrödinger equation *Preprint* quant-ph/9801031
[4] Fröman N and Fröman P O 1965 *JWKB Approximation. Contribution to the Theory* (Amsterdam: North-Holland)
[5] Graffi S, Grecchi V and Simon B 1970 *Phys. Lett.* B **32** 631
[6] Simon B and Dicke A 1970 *Ann. Phys., NY* **58** 76
[7] Bender C M and Wu T T 1969 *Phys. Rev.* **184** 1231
Bender C M and Wu T T 1973 *Phys. Rev.* D **7** 1620
[8] Loeffel J J, Martin A, Simon B and Wightman A S 1969 *Phys. Lett.* B **30** 656
[9] Horzela A 1986 *Acta Phys. Pol.* B **17** 425
[10] Čizek J and Vrscay E R 1984 *Phys. Rev.* A **30** 1550
[11] Giller S 1989 *J. Phys. A: Math. Gen.* **22** 2965
[12] Giller S 1990 *Acta Phys. Pol.* B **21** 675–709
[13] Eden R J, Landshoff P V, Olive D I and Polkinghorn J C 1966 *The Analytic S-Matrix* (Cambridge: Cambridge University Press)
[14] Zinn-Justin J 1977 *Salamanca 1977* (*Lecture Notes in Physics vol 126)* ed J A Azcerraga (Berlin: Springer) p 77
Zinn-Justin J 1981 *Phys. Rep.* **70** 109
[15] Carlitz R N and Nicole D A 1985 *Ann. Phys., NY* **164** 411
Carlitz R N 1984 *Pittsburgh preprint* PITT-19-84
[16] Nicole D A and Walters P J 1988 *J. Phys. A: Math. Gen.* **21** 2351
[17] Millard P A 1985 *Nucl. Phys.* B **259** 266
[18] Garrison J C and Wright E M 1985 *Phys. Lett.* A **108** 129
[19] Voros A 1983 *Ann. Inst. Henri Poincaré* A **39** 211
[20] Berry M V 1988 *Proc. R. Soc.* A **422** 7
[21] Berry M V 1990 *Proc. R. Soc.* A **427** 241
[22] Silverstone H 1985 *Phys. Rev. Lett.* **55** 2523–6
[23] Berry M V and Howls C J 1990 *Proc. R. Soc.* A **430** 653–67
Berry M V and Howls C J 1991 *Proc. R. Soc.* A **434** 657–75
[24] Daalhuis Olde A B 1998 *Proc. R. Soc.* A **445** 1–29
[25] Delabaere E, Dillinger H and Pham F 1997 *J. Math. Phys.* **38** 6126–84
[26] Delabaere E and Pham F Resurgent methods in semiclassical asymptotics *Ann. Inst. Henri Poincaré Phys. Theor.* at press
[27] Ecalle J Cinq application des fonctions resurgentes *Publ. Math. D'Orsay* (Orsay: Universite Paris-Sud)
Ecalle J 1994 Weighted products and parametric resurgence *Analyse Algebrique des Perturbations Singulieres I: Methodes Resurgentes Travaux en Course* (Paris: Hermann) pp 7–49
[28] Sternin B and Shatalov V 1996 *Borel–Laplace Transform and Asymptotic Theory* (Boca Raton, FL: CRC Press)
[29] Fröman N and Fröman P O 1998 *J. Math. Phys.* **39** 4417–29
[30] Balian R, Parisi G and Voros A 1979 *Feynman Path Integrals (Lecture Notes in Physics vol 106)* (Berlin: Springer) p 337
[31] Landau L D and Lifshitz E M 1965 *Quantum Mechanics. Nonrelativistic Theory* (Oxford: Pergamon)
[32] Bateman H 1953 *Higher Transcendental Functions* (New York: McGraw-Hill) p 100 (formula (12))
[33] Joye A and Pfister C-H 1993 *J. Math. Phys.* **34** 454–79
[34] Hagedorn G A and Joye A 1998 *Ann. Inst. Henri Poincare. Phys. Theor.* **68** 85–134
[35] Combes J-M and Hislop P D 1991 *Commun. Math. Phys.* **140** 291–320
[36] Bentosela F and Grecchi V 1991 *Commun. Math. Phys.* **142** 169–92
[37] Fedoryuk M V 1983 *Asymptotic Methods for Linear Ordinary Differential Equations* (Moscow: Nauka) (in Russian)